Geophys. J. Int. (2004) **157,** 381–398 doi: 10.1111/j.1365-246X.2004.02222.x

Present-day crustal deformation and plate kinematics in the Middle East constrained by GPS measurements in Iran and northern Oman

Ph. Vernant,[1]* F. Nilforoushan,[2] D. Hatzfeld,[3] M. R. Abbassi,[4] C. Vigny,[5] F. Masson,[1] H. Nankali,[2] J. Martinod,[3] A. Ashtiani,[4] R. Bayer,[1] F. Tavakoli[2] and J. Chéry[1]

[1]*Laboratoire Dynamique de la Lithosphère, Université Montpellier II - CNRS, Pl. E. Bataillon,* 34095 *Montpellier Cedex* 05, *France*
[2]*Geodynamic Department, National Cartographic Center,* PO Box 13185-1684, *Meraj Ave. Tehran, Iran*
[3]*Laboratoire de Géophysique Interne et Tectonophysique, Université Joseph Fourrier Grenoble - CNRS, BP* 53, 38041 *Grenoble Cedex* 9, *France*
[4]*International Institute of Earthquake Engineering and Seismology, Farmanieh, Dibaji, Arghavan St., N°* 27 19531 *Tehran, Iran*
[5]*Laboratoire de Géologie, Ecole Normale Supérieure - CNRS,* 24 *rue Lhomond,* 75231 *Paris Cedex* 05, *France*

Accepted 2003 December 11. Received 2003 November 28; in original form 2003 April 10

SUMMARY

A network of 27 GPS sites was implemented in Iran and northern Oman to measure displacements in this part of the Alpine–Himalayan mountain belt. We present and interpret the results of two surveys performed in 1999 September and 2001 October. GPS sites in Oman show northward motion of the Arabian Plate relative to Eurasia slower than the NUVEL-1A estimates (e.g. 22 $\pm$ 2 mm yr^{-1} at N8° $\pm$ 5°E instead of 30.5 mm yr^{-1} at N6°E at Bahrain longitude). We define a GPS Arabia–Eurasia Euler vector of 27.9° $\pm$ 0.5°N, 19.5° $\pm$ 1.4°E, 0.41° $\pm$ 0.1° Myr^{-1}. The Arabia–Eurasia convergence is accommodated differently in eastern and western Iran. East of 58°E, most of the shortening is accommodated by the Makran subduction zone (19.5 $\pm$ 2 mm yr^{-1}) and less by the Kopet-Dag (6.5 $\pm$ 2 mm yr^{-1}). West of 58°E, the deformation is distributed in separate fold and thrust belts. At the longitude of Tehran, the Zagros and the Alborz mountain ranges accommodate 6.5 $\pm$ 2 mm yr^{-1} and 8 $\pm$ 2 mm yr^{-1} respectively. The right-lateral displacement along the Main Recent Fault in the northern Zagros is about 3 $\pm$ 2 mm yr^{-1}, smaller than what was generally expected. By contrast, large right-lateral displacement takes place in northwestern Iran (up to 8 $\pm$ mm yr^{-1}). The Central Iranian Block is characterized by coherent plate motion (internal deformation $<$2 mm yr^{-1}). Sites east of 61°E show very low displacements relative to Eurasia. The kinematic contrast between eastern and western Iran is accommodated by strike-slip motions along the Lut Block. To the south, the transition zone between Zagros and Makran is under transpression with right-lateral displacements of 11 $\pm$ 2 mm yr^{-1}.

Key words: GPS, intracontinental deformation, Iran, Middle East, plate kinematics, subduction.

1 INTRODUCTION

Iran (Fig. 1) is an ideal natural laboratory for studying the kinematics and dynamics of plate interactions because of the various tectonic processes encountered, including continental collision (Zagros, Caucasus, Alborz, Kopet-Dag, Talesh), subduction of oceanic lithosphere (Makran) and a sharp transition between a young orogen (Zagros) and a subduction zone (Makran).

The geodynamics (Fig. 1) of the region is dominated by the convergence between the Arabian and Eurasian plates (Jackson & McKenzie 1984, 1988). According to the NUVEL-1A plate tectonic model (DeMets *et al.* 1990, 1994), based on analysis of global seafloor spreading, fault systems and earthquake slip vectors, the Arabian Plate is moving N13°E at a rate of about 31 mm yr^{-1} relative to Eurasia at the longitude of 52°E. Geodetic data (e.g. Sella *et al.* 2002; Kreemer *et al.* 2003; McClusky *et al.* 2003) suggest roughly the same orientation but with rates $\sim$10 mm yr^{-1} lower. This convergence involves intracontinental shortening everywhere in Iran except its southern margin, east of about 58°E, where the Oman Sea subducts northward under the Makran (Byrne *et al.* 1992). The historical (Ambraseys & Melville 1982) and instrumental seismicity (Engdahl *et al.* 1998) in Iran suggests an intracontinental deformation concentrated in several mountain belts surrounding relatively aseismic blocks (Central Iran, Lut and South Caspian blocks, Fig. 2). The Arabia–Eurasia convergence takes place first in southern Iran

*Corresponding author: CNRS/LDL, ISTEEM Université Montpellier II, Case Courrier 060, 4 place E. Bataillon. E-mail: vernant@dstu.univ-montp2.fr

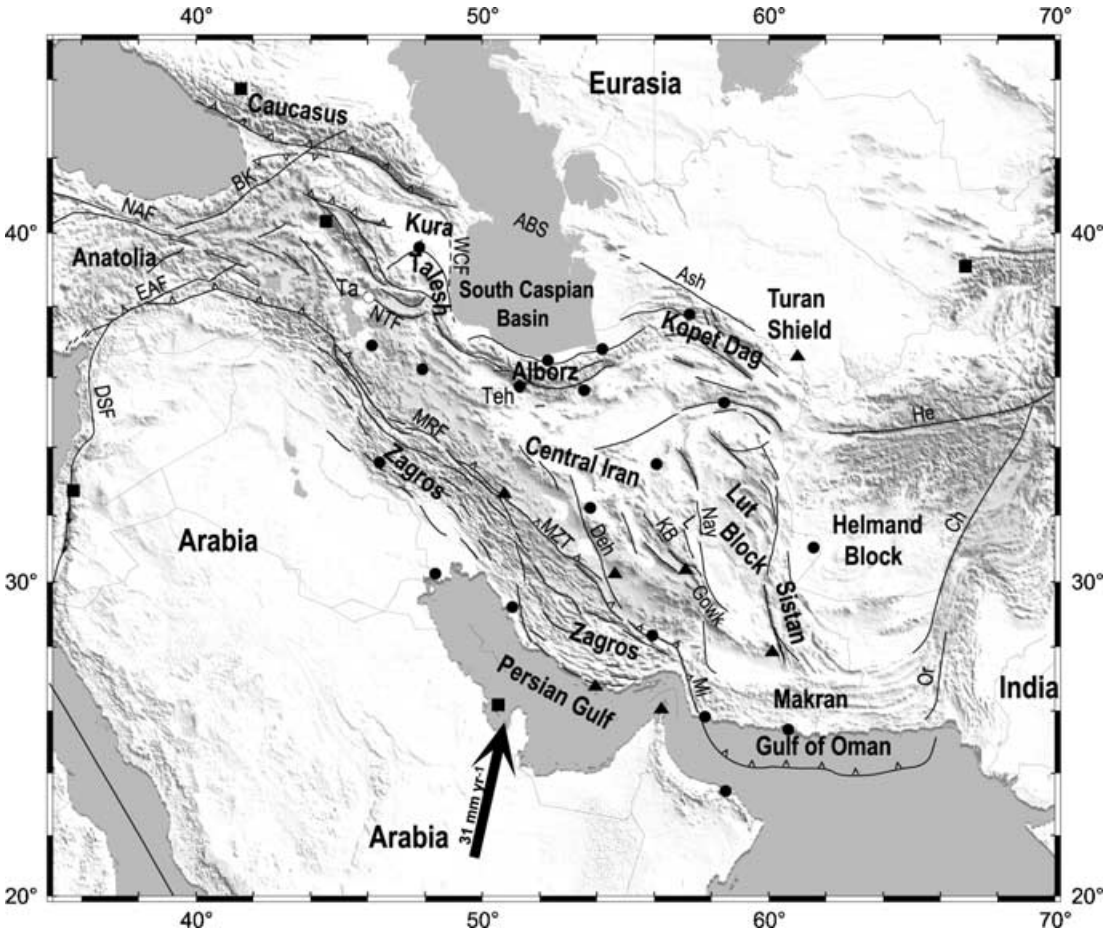

Figure 1. Simplified tectonic map of the Middle East region superimposed on topography. The heavy arrow shows NUVEL-1A plate motion relative to Eurasia. Black circles and triangles, GPS sites in this study (respectively with forced centring or tripod); black squares, IGS stations. Ta: Tabriz, Teh: Tehran, NAF: North Anatolian Fault, EAF: East Anatolian Fault, ABS: Apsheron Balkan Sills, Ash: Ashkabad Fault, BK: Borzhomi-Kazbeg, Ch: Chaman Fault, Deh: Dehshir Fault, He: Herat Fault, Kura: Kura Basin, KB: Kuh Banan Fault, L: Lakarkuh Fault, MRF: Main Recent Fault, MZT: Main Zagros Thrust, Mi: Minab Zendan Palami fault zone, Nay: Nayband Fault, NTF: North Tabriz Fault, Or: Ornach-Nal Fault, WCF: West Caspian Fault.

with the Zagros fold and thrust belt (Fig. 1) that started as early as end Eocene (Hessami *et al.* 2001). However, the climax of orogeny indicated by the Alborz and Zagros uplift and South Caspian subsidence took place during the late Neogene subsequent to the complete closure of the Neo-Tethyan ocean (e.g. Stöcklin 1968; Falcon 1974; Berberian & King 1981; Berberian *et al.* 1982; Berberian 1983, 1995; Alavi 1994). Compressional structures in this range are striking obliquely to the convergence direction (especially in the central and northern part). This is probably due to partitioning between thrusting and strike-slip on major faults such as the Main Recent Fault in northern Zagros (Jackson 1992; Talebian & Jackson 2002). North of the Zagros, the Central Iranian Block is believed to be rigid (Jackson & McKenzie 1984), and part of the deformation is transmitted to the north in the Alborz (also Elburz), Talesh and Caucasus mountains (Fig. 1). The Alborz and Talesh mountains are surrounding the western and southern border of the South Caspian Block. The regular occurrence of large historical earthquakes in Alborz suggests an important deformation of this mountain belt north of Tehran. East of the South Caspian Block, the Kopet-Dag is accommodating part of the Arabia–Eurasia convergence not absorbed by the Makran subduction. South of the Kopet-Dag belt, the Lut Block is bordered to the west and east by large strike-slip faults (Conrad *et al.* 1982; Tirrul *et al.* 1983; Nowroozi & Mohajer-Ashjai 1985; Walker & Jackson 2002). Large strike-slip motion is also reported along the Minab–Zendan–Palami fault zone that corresponds to the transition zone between the Zagros collision and Makran subduction (also the Oman Line) (Haynes & McQuillan 1974; Stöcklin 1974; Falcon 1976; Kadinsky-Cade & Barazangi 1982).

To date, except in the central Zagros (Tatar *et al.* 2002), no direct measurements of the deformation rates have been performed in Iran. The available estimations are based on different assumptions such as the velocities of the Arabian Plate given by NUVEL-1 (DeMets *et al.* 1990) or geomorphic observations with ages which are not well constrained. Using recent and historical seismicity, fault plane solutions and geomorphic analysis of young structures visible on satellite images, Jackson & McKenzie (1984, 1988), Jackson (1992) and Jackson *et al.* (2002), developed a plate tectonic framework to understand the deformation in the Middle East and eastern Mediterranean. They suggested that Iran is pushed against its northeastern (Turan Shield) and eastern (Helmand Block) boundaries and so considerable crustal shortening must take place in the Kopet-Dag (about 15 mm yr^{-1} according to Lyberis & Manby 1999). They proposed that 10 to 15 mm yr^{-1} are accommodated by the Zagros and 15 to 20 mm yr^{-1} by the Alborz. According to these values, the seismic strain released in these belts with respect to the total strain would be less than 15 per cent for Zagros and 50 to 100 per cent for Alborz

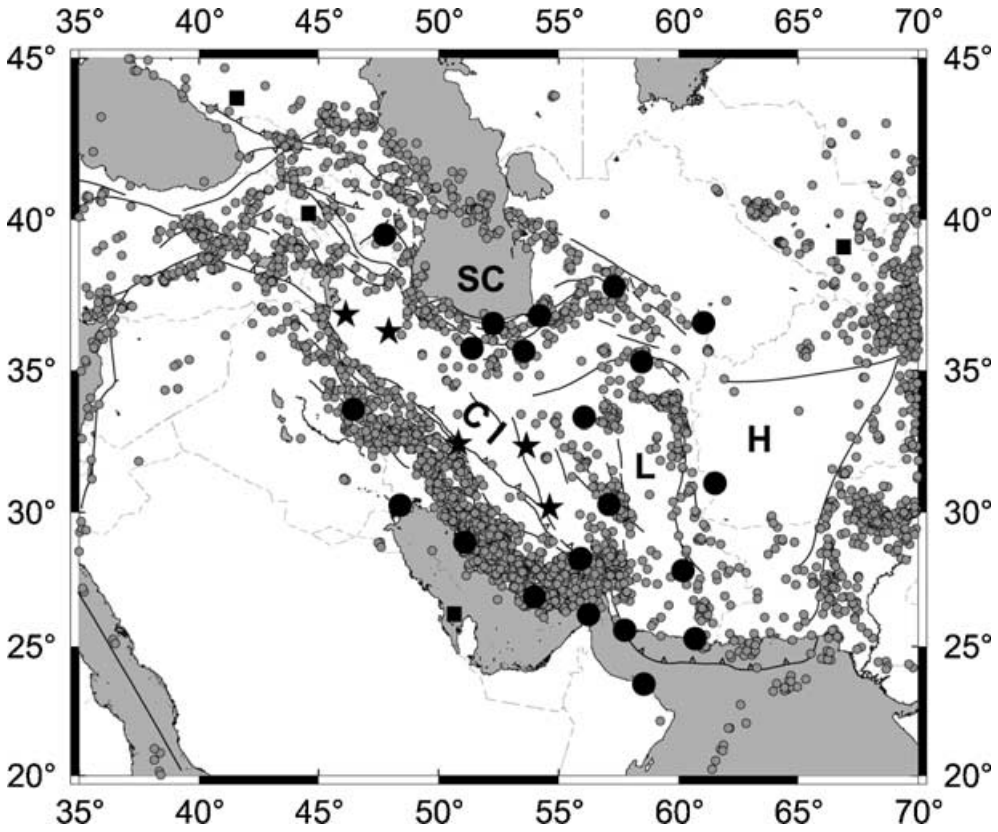

Figure 2. Seismicity of Iran 1964–98, from Engdahl *et al.* (1998). CI: Central Iran, H: Helmand Block, L: Lut Block, SC: South Caspian Block. Black circles, GPS sites; black stars, GPS sites used to define the Central Iranian Block; black squares, IGS stations.

(Jackson & McKenzie 1988). They suggested that the prolongation of the right-lateral motion between Anatolia and Eurasia is mainly accommodated by the Main Recent Fault at a rate of 10–17 mm yr^{-1} (Talebian & Jackson 2002).

We implemented a GPS network in Iran to improve our knowledge of the present-day kinematics of the Alpine–Himalayan mountain belt and the deformation of the young Iranian orogens. Two GPS surveys were performed in 1999 and 2001. We present the GPS-derived velocity field from these measurements and consider the implications of observed motions on the motion of the Arabian Plate and the kinematics of the plate interactions in the Middle East. The average benchmark spacing is about 300 km, therefore our conclusions are mainly related to large tectonic structures.

2 DATA ACQUISITION AND PROCESSING

We initiated GPS measurements in Iran and northern Oman in 1999 September and observed the network again in 2001 October (Nilforoushan *et al.* 2003). For both surveys we used Ashtech Z12 and Trimble 4000-SSI receivers with choke ring antennas during four 24-hr sessions. Among the 25 sites which were implemented in Iran (Fig. 1), 18 are on concrete pillars (forced centring) and 7 are observed using tripods (see Nilforoushan *et al.* 2003, for details). Two other sites are located in northern Oman (Fig. 1). Based on previous studies on strain accumulation across the faults (e.g. Savage & Burford 1973; Wright *et al.* 2001), we install most of sites far enough (50 km) from active faults to avoid measuring transient deformation related to the seismic cycle. During 2002 September two sites in northwestern Iran were remeasured (sites DAMO and MIAN, Fig. 4). To strengthen the reference frame and aid in orbit determination we included in our analysis data from up to ∼150 globally distributed stations from the International GPS Service (IGS) (Beutler *et al.* 1993) acquired between 1995 January and 2002 December. Global solutions were performed by the Scripps Orbit and Permanent Array Center (SOPAC) (Bock *et al.* 1997) (solutions available at http://sopac.ucsd.edu).

In order to obtain precise site coordinates, we analysed data using the GAMIT/GLOBK software (Herring 2002; King & Bock 2002) in a three-step approach (Feigl *et al.* 1993; Oral 1994; Dong *et al.* 1998). During the first step we applied loose *a priori* constraints to all parameters and used doubly differenced GPS phase observations from each day to estimate stations coordinates, the zenith delay of atmosphere at each station every 2 hr, and the orbital and Earth orientation parameters (EOP). We included in this analysis the observations of ∼17 IGS stations in order to link our regional observations to the global GPS network. From this first step, we extract the repeatabilities (i.e. the rms of the daily independent measurement about their mean value; Larson & Agnew 1991). This gives a first idea of the short-term precision of the measurements. Fig. 3 presents these repeatabilities; the mean values for north, east and vertical components for the Iranian network baselines for the 1999 survey are respectively 1.1, 1.4 and 3.7 mm and 0.9, 1.2 and 2.3 mm for the 2001 survey (see Nilforoushan *et al.* 2003, for details). In a second step, we estimated a consistent set of coordinates and velocities using the daily loosely constrained estimates of station coordinates, orbits and EOP and their covariance as quasi-observations in a Kalman filter. During this step we combined our regional observations with the global (SOPAC data) quasi-observations. The daily

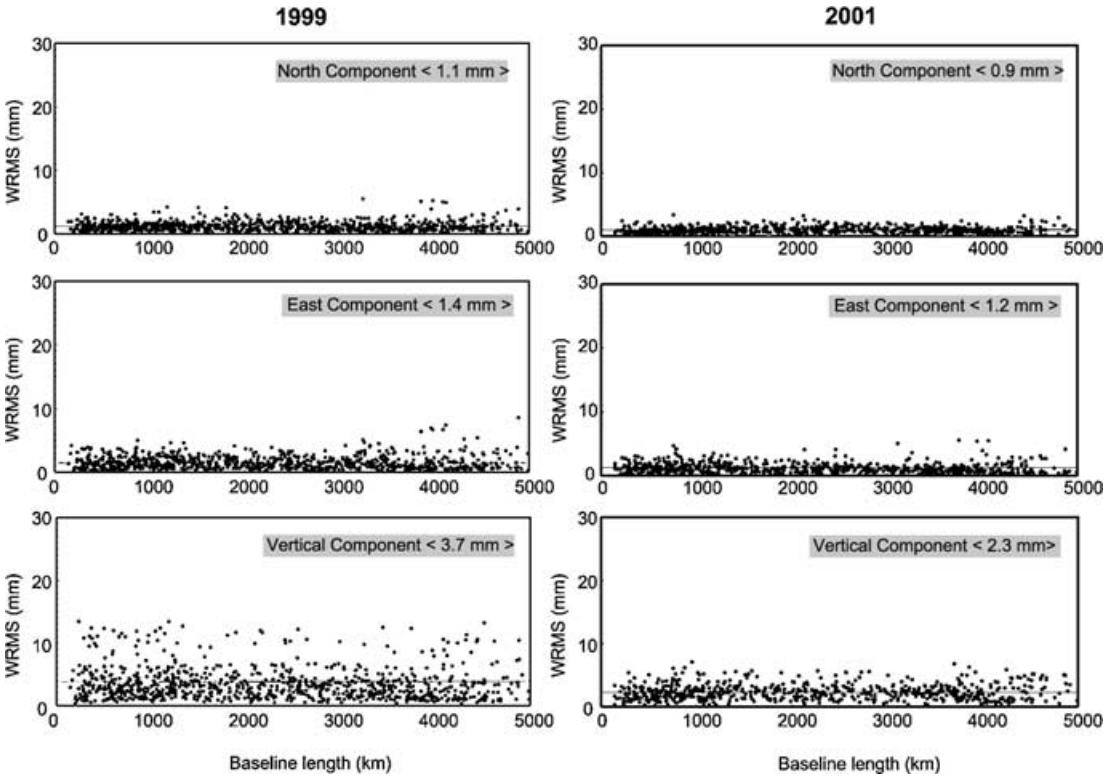

Figure 3. Baseline component repeatabilities versus baseline length. First, second and third rows are for north, east and vertical components. Values indicated are the average for the shortest baselines.

analyses of SOPAC were combined in 30-day averages when no surveys occurred during this time. In a third step we applied generalized constraints (Dong *et al.* 1998) while estimating a six-parameter transformation (rate of change of translation and rotation).

To compute the velocities relative to the stable Eurasia, we tested three different approaches. First, we followed McClusky *et al.* (2000) and defined the Eurasian frame by minimizing the horizontal velocities of 16 IGS stations in western Europe and central Asia (Table 1). The root mean square (rms) departure of the velocities of the 16 IGS stations after transformation was 0.4 mm yr^{-1}. Second, we constrained the velocities of 31 IGS stations to their ITRF2000 (Altamimi *et al.* 2002) values and we subtracted the motions generated by the rotation of the Eurasian Plate described by the NNR-NUVEL-1A model (DeMets *et al.* 1994). It produced a global fit of 0.5 mm yr^{-1} to ITRF2000, but the residual velocities of the IGS stations on the Eurasian Plate remain high (Nilforoushan *et al.* 2003). Third, we removed to our velocity field in the ITRF2000 reference frame the motions generated by the Eurasian Plate defined by Altamimi *et al.* (2002). The mean value of the differences between the Eurasian velocities obtained by the first and third approaches is 0.44 mm yr^{-1} with rms of 0.23 mm yr^{-1}. Therefore, the use of NNR-NUVEL-1A does not seem to be appropriate to define a Eurasian reference frame, at least for the short timescale we consider.

In order to easily compare our velocity field with the results of McClusky *et al.* (2000), we present the velocities obtained by the first method (Fig. 4). The GPS velocities relative to Eurasia are listed in Table 1 together with the 1σ uncertainties. The rotation pole obtained for the Eurasian Plate in the ITRF2000 reference frame is given at the end of Table 1. Defining real uncertainties is not a trivial problem, especially because only two surveys were conducted. Indeed, error spectra of GPS data are spatially correlated because of common orbital, Earth rotation and regional atmospheric errors (Feigl *et al.* 1993). Moreover, errors are also temporally correlated due to apparent or real motions related to atmospheric disturbance, monument instability and orbital misfits (Zhang *et al.* 1997; Mao *et al.* 1999). Times-series for the site BAHR are a good example of these large variations (Fig. 5a), which are especially visible on the east component (± 8 mm). Fortunately, most of the times-series of the permanent stations used display lower variations, with amplitudes similar to those observed for the north component of the BAHR site (e.g. station ZECK, Fig. 5a). By removing a common mode component within a region, as we do implicitly in estimating relative velocities, we reduce the magnitude of the coloured noise and whiten the noise. In addition of the error in station position estimates which are assumed to be random, we added a random walk component equal to 2 mm $yr^{-1/2}$ to take into account the coloured noise and deal with a possible monument instability (Langbein & Johnson 1997). We used the three-times-surveyed sites in northwestern Iran (DAMO and MIAN) to compute time-series of station positions. They were computed using the same approach as for the velocity solution except that we treated each set of quasi-observations independently. We defined the reference frame at each epoch by minimizing the adjustments of horizontal positions for all stations from values estimated from the velocity solution. The daily estimates were combined into a single set of quasi-observations for each survey to better assess the long-term statistic. Fig. 5(b) shows the detrended residual series for these stations. The velocities of DAMO and MIAN do not differ significantly from the solution of Nilforoushan *et al.* (2003) and the three surveys are quite well lined up. Another estimation of the uncertainty is to apply external knowledge that does not depend on the knowledge of the full error spectrum. For the five sites on the

Table 1. GPS site velocities and 1σ uncertainties. Latitude (Lat.) and longitude (Lon.) are given in degrees north and east, respectively. Velocities and uncertainties are given in mm yr^{-1}. The Eurasian frame is determined following the approach of McClusky *et al.* (2000), by minimizing the adjustments to the horizontal velocities of the 16 stations given at the end of the table. *A priori* velocities for Eurasian stations were set to zero except for POL2 and KIT3 (*a priori* velocity of 2 mm yr^{-1} N and 0.5 mm yr^{-1} E).

Site	Lon.	Lat.	E vel.	E σ^a	N vel.	N σ^a	ρEN^b
Middle East sites							
ALIS	51.082	28.919	1.25	1.68	20.96	1.51	0.011
ARDA	53.822	32.313	0.27	1.61	14.66	1.49	0.015
BAHR*	50.608	26.209	2.97	0.91	22.07	0.88	0.039
BAZM	60.180	27.865	5.22	2.05	3.37	1.63	0.025
BIJA	47.930	36.232	−1.09	1.75	14.64	1.55	0.015
CHAB	60.694	25.300	1.14	1.89	7.96	1.57	0.022
DAMO	47.744	39.513	7.00	1.33	15.78	1.26	0.016
ELRO*	35.771	33.182	−3.70	1.43	10.84	1.41	0.004
HAJI	55.800	28.330	3.49	1.82	15.95	1.60	0.016
HARA	54.608	30.079	2.16	1.71	16.26	1.52	0.019
ILAM	46.427	33.648	−0.80	1.68	17.86	1.51	0.015
JASK	57.767	25.636	2.78	1.70	14.56	1.49	0.023
KASH	58.464	35.293	1.13	1.65	6.33	1.51	0.019
KATZ*	35.688	32.995	−4.04	1.39	11.34	1.38	0.004
KERM	57.119	30.277	1.67	2.51	16.43	1.71	0.033
KHAS	56.233	26.208	5.14	1.93	24.60	1.57	0.022
KHOS	48.409	30.246	−0.09	1.71	18.91	1.53	0.012
KORD	54.199	36.860	−0.89	1.74	6.31	1.54	0.021
KSHA	51.255	34.150	9.89	1.67	10.71	1.52	0.016
LAMB	54.004	26.883	2.90	2.01	22.49	1.59	0.019
MAHM	52.285	36.588	−2.39	1.61	6.22	1.54	0.020
MIAN	46.162	36.908	−1.57	1.33	13.88	1.25	0.015
MUSC	58.569	23.564	7.67	1.77	26.09	1.54	0.019
NSSP*	44.503	40.226	2.21	1.13	8.09	1.11	0.024
ROBA	56.070	33.369	2.13	1.67	11.77	1.51	0.018
SEMN	53.564	35.662	0.10	1.72	9.83	1.53	0.021
SHAH	50.748	32.367	−0.05	1.63	14.09	1.50	0.012
SHIR	57.308	37.814	2.11	1.74	3.65	1.52	0.023
TEHR	51.386	35.747	0.61	1.73	14.03	1.56	0.012
YAZT	61.034	36.601	3.14	1.71	0.91	1.53	0.020
ZABO	61.517	31.049	1.72	1.65	0.97	1.50	0.022
ZECK*	41.565	43.788	0.24	0.94	0.87	0.95	0.008
Eurasian and Central Asian sites used to define Eurasian fixed reference frame							
BOR1*	17.073	52.277	0.30	0.73	0.05	0.73	0.000
BRUS*	4.359	50.798	−0.10	0.71	−1.08	0.71	0.000
GRAZ*	15.493	47.067	0.63	0.71	−0.44	0.71	−0.001
HERS*	0.336	50.867	−0.18	0.66	1.40	0.65	−0.001
JOZE*	21.032	52.097	−0.22	0.73	0.16	0.73	−0.001
KIT3*	66.885	39.135	0.46	0.53	1.22	0.53	0.001
KOSG*	5.810	52.178	−0.55	0.68	0.52	0.68	0.000
METS*	24.395	60.217	0.30	0.72	−0.94	0.72	0.000
NYAL*	11.865	78.930	−0.03	0.52	−0.66	0.51	0.000
ONSA*	11.926	57.395	−0.81	0.69	−0.06	0.69	0.000
POL2*	74.694	42.680	0.23	0.51	3.07	0.51	0.000
POTS*	13.066	52.379	−0.05	0.69	0.09	0.69	0.000
TROM*	18.938	69.663	−0.60	0.64	1.19	0.64	−0.001
WTZR*	12.879	49.144	0.19	0.72	−0.04	0.72	−0.001
ZIMM*	7.465	46.877	0.61	0.70	−0.18	0.70	−0.001
ZWEN*	36.759	55.699	0.57	0.69	0.10	0.68	−0.001
Rotation pole of Eurasia (in ITRF2000 frame)							
Plate	Lat. (°N)		Lon. (°E)		Rate (° Myr^{-1})		Reference
EURA	56.11 ± 1.4		−100,79 ± 1.9		0.26 ± 0.01		This study

[a] 1σ uncertainties.
[b] Correlation coefficient between the east and north uncertainties.
*Permanent stations available by ftp at: lox.ucsd.edu.

Central Iranian Block which have relatively little internal deformation the residuals are all inside the 1σ uncertainties (*cf.* section 3.2). Hence, problems can come from large site displacements during the survey. As the major number of the sites are on concrete pillars, this allows a quite good confidence in the 1999–2001 results and their uncertainties (see Nilforoushan *et al.* 2003, for details). In addition, our computed velocities of IGS stations are in good agreement with other values given by McClusky *et al.* (2000) or

Table 2. Euler vectors for Arabia–Eurasia (Ar–Eu). Counter-clockwise rotation is positive. Uncertainties are 1σ.

Plate pair	Lat. (°N)	Long. (°E)	Rate (° Myr^{-1})	Reference and comments
Ar–Eu	27.9 ± 0.5	19.5 ± 1.4	0.41 ± 0.1	This study
Ar–Eu	25.6 ± 2.1	19.7 ± 4.1	0.50 ± 0.1	McClusky *et al.* (2000)
Ar–Eu	27.4 ± 1.0	18.4 ± 2.5	0.40 ± 0.04	McClusky *et al.* (2003)
Ar–Eu	26.29 ± 2.1	22.82 ± 1.1	0.427 ± 0.029	Sella *et al.* (2002)
Ar–Eu	23.0	7.9	0.26	Kreemer *et al.* (2000)
Ar–Eu	26.2 ± 0.9	20.4 ± 3.7	0.437 ± 0.023	Kreemer *et al.* (2003)
Ar–Eu	24.6 ± 1.6	13.7 ± 3.9	0.50 ± 0.5	DeMets *et al.* (1994)

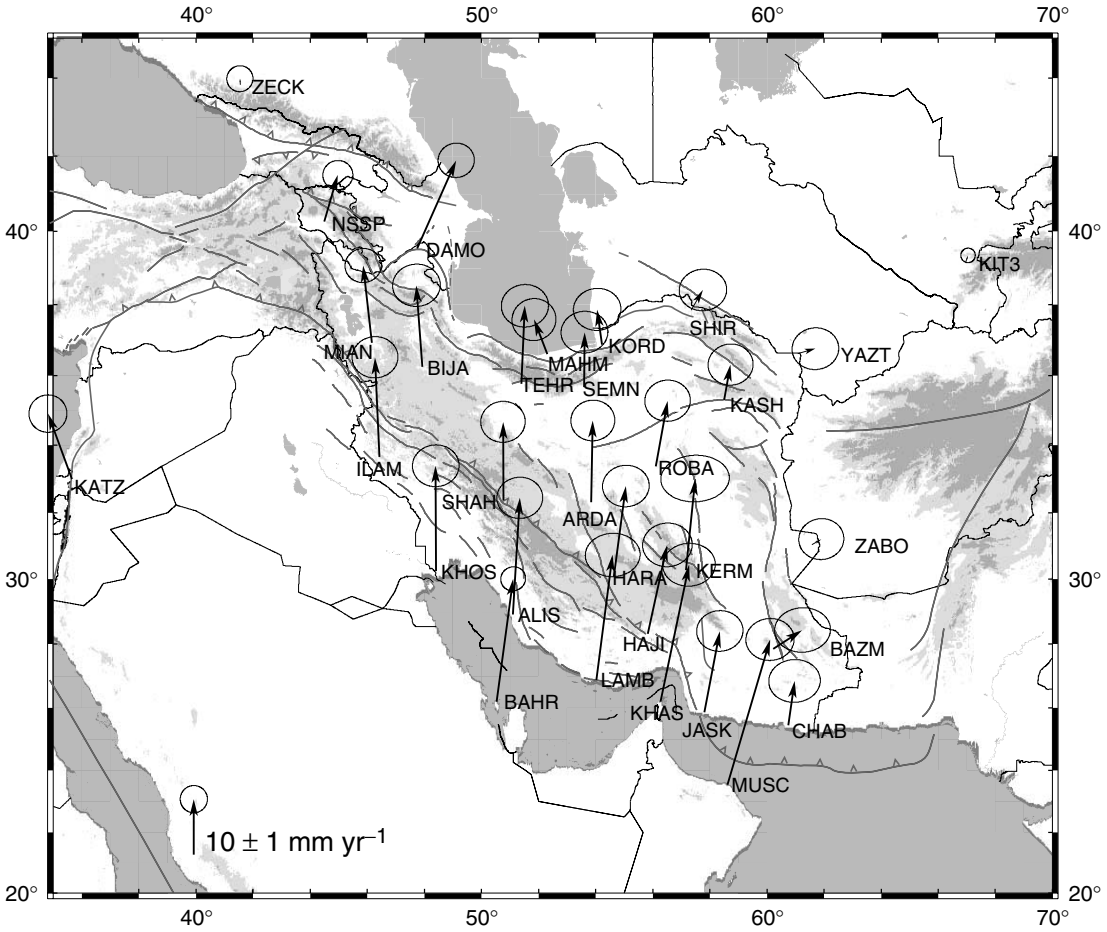

Figure 4. GPS horizontal velocities and their 95 per cent confidence ellipses in Eurasia-fixed reference frame for the period 1999–2001. Tectonic symbols are the same as in Fig. 1.

Wang *et al.* (2001) (see Figs 10 and 12 and Nilforoushan *et al.* 2003).

3 VELOCITY FIELD

3.1 Arabian Plate rotation

We performed several tests to define an Arabia–Eurasia Euler vector using the results of our study (sites KHAS, KHOS and MUSC and the permanent stations of BAHR and KATZ, Fig. 7) and the results of the McClusky *et al.* (2003) study (sites KIZ2, KRCD and GAZI, Fig. 7). The different solutions of the Arabia–Eurasia Euler vector (i.e. adding or not the sites of McClusky *et al.* 2003, and removing some of our sites) were slightly similar. We did not finally include the site KATZ in the computation due to its position very close to the Dead Sea Fault. We present the solution obtained with the sites KHAS, KHOS, MUSC and BAHR, and the three sites of the McClusky *et al.* (2003) study. Except for one study (Kreemer *et al.* 2000) which found a pole closer to NUVEL-1A but with a much smaller rate, the result (Table 2 and Fig. 6) is consistent with previous studies based on spatial geodetic data (Sella *et al.* 2002; Kreemer *et al.* 2003; McClusky *et al.* 2003), but with a slightly smaller uncertainty due to the better sampling location of the benchmarks. The rms on the residual velocities of the Arabian Plate is 0.9 mm yr^{-1}. This and the low seismicity level indicate that the internal deformation of the northern part of Arabian Plate is less than

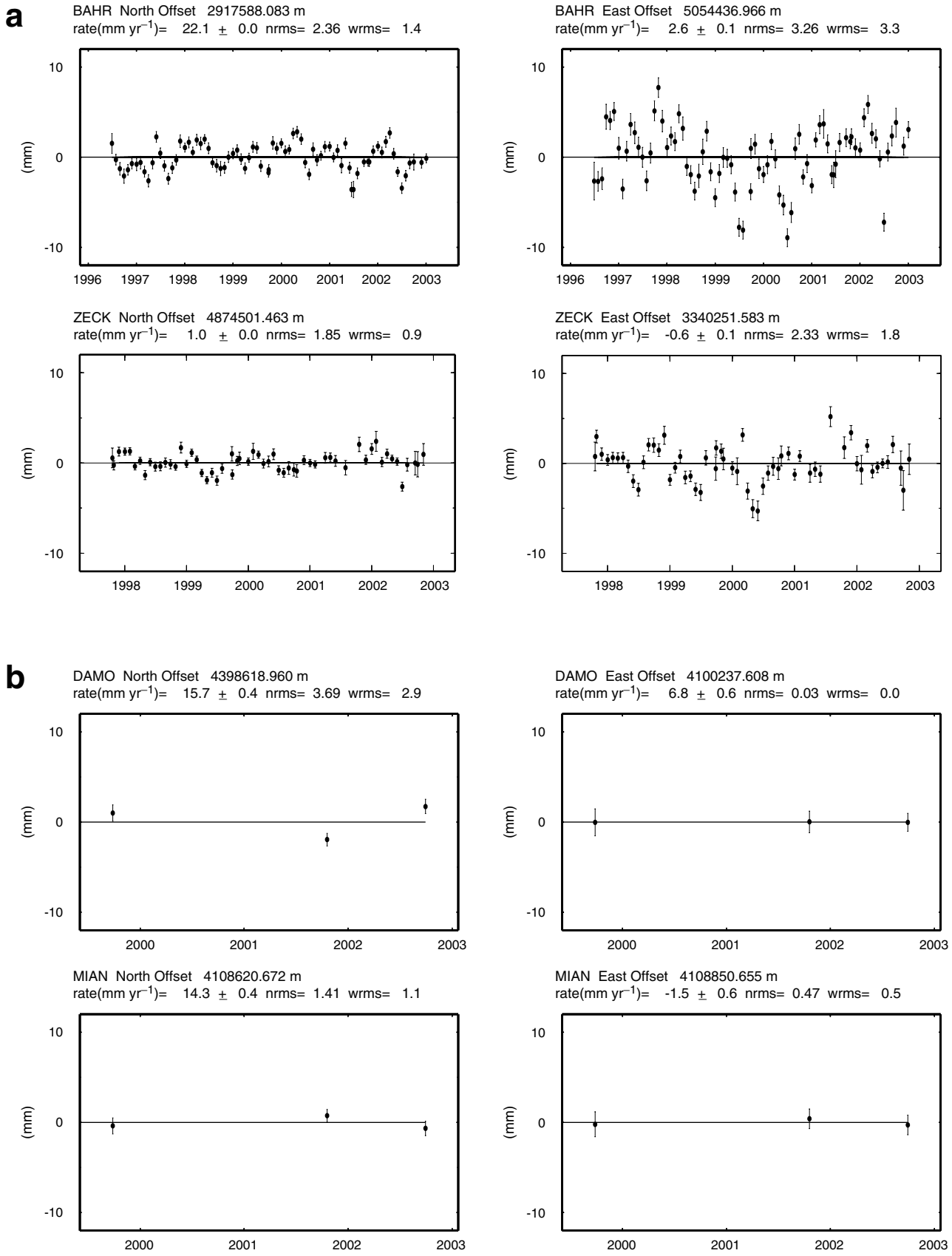

Figure 5. Time series of geocentric position of stations at (a) Bahrain (BAHR) and (b) sites DAMO and MIAN after removing the best fit straight line. Labels show estimated rate with respect to the Eurasia, its 1σ uncertainty, and the normalized (nrms) and weighted (wrms) root mean square scatters (in mm). The uncertainty does not reflect the random walk process noise added to the solution (see text).

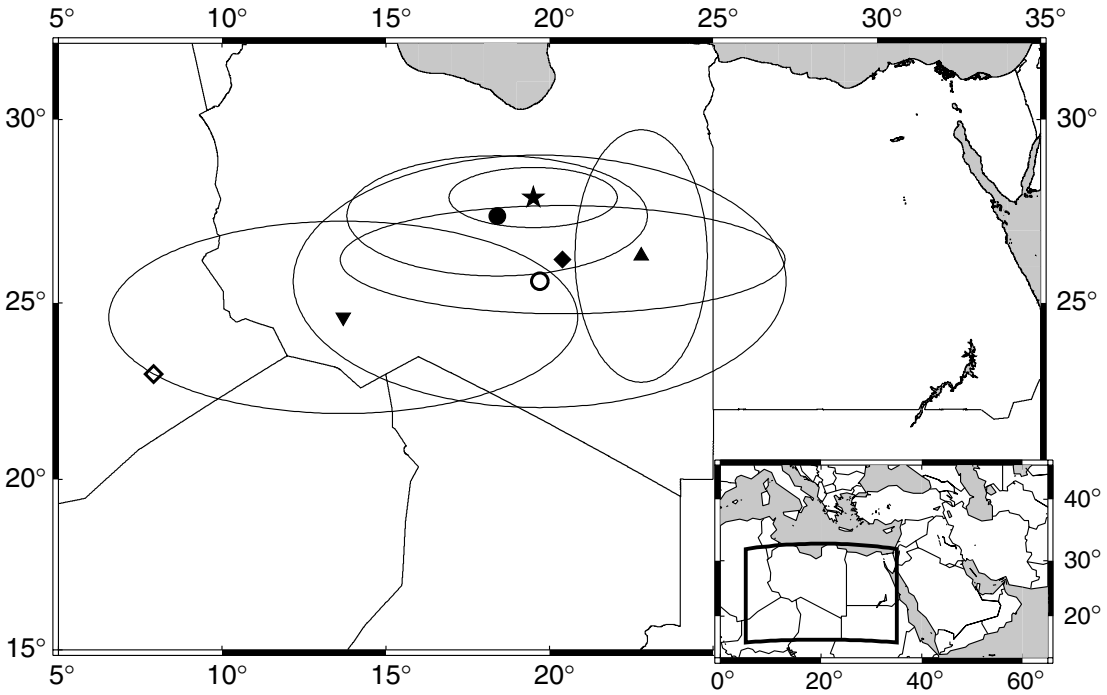

Figure 6. Poles of rotation for Arabia relative to Eurasia and 95 per cent confidence limits. The star indicts the result of this study; the circles are for McClusky *et al.* (2000) (white) and McClusky *et al.* (2003) (black); the triangle is for Sella *et al.* (2002); the diamonds are for Kreemer *et al.* (2000) (white) and Kreemer *et al.* (2003) (black); the inverted triangle is for NNR-NUVEL-1A (DeMets *et al.* 1994).

Table 3. Euler vectors for central Iran–Eurasia (Ir–Eu). Counter-clockwise rotation is positive. Uncertainties are 1σ.

Plate pair	Lat. (°N)	Long. (°E)	Rate (° Myr^{-1})	Reference and comments
Ir–Eu	23.15 ± 13.2	0.98 ± 1.2	0.189 ± 0.1	This study
Ir–Eu	27.5	65.8	0.56	Jackson & McKenzie (1984)

2 mm yr^{-1}. Therefore, the usual assumption of a rigid Arabian Plate seems appropriate, at least for its northern part. The NUVEL-1A model (DeMets *et al.* 1990, 1994) derived from analyses of sea-floor magnetic anomalies, transform fault orientations, and global circuit closure provides an Arabia–Eurasia Euler vector determined over the last 3 Myr. Although the directions of our vectors are not so far from the NUVEL-1A directions, the GPS convergence rate is systematically ∼10 mm yr^{-1} lower in the Persian and Oman gulfs (e.g. 22 ± 2 mm yr^{-1} at N8° ± 5°E instead of 30.5 mm yr^{-1} at N6°E for Bahrain, and 25 ± 2 mm yr^{-1} at N12° ± 5°E instead of 35 mm yr^{-1} at N7°E for the Strait of Hormuz). Sella *et al.* (2002) suggested a gradual slowing of the Arabian Plate due to the collision with Eurasia and the increase of the gravitational body forces induced by the thickening of the Zagros and Caucasus. However, on the basis of a re-examination of the Red Sea opening, Chu & Gordon (1998) found significant differences between NUVEL-1A and recent studies (McQuarrie *et al.* 2003), suggesting a fairly constant rate (∼2–3 cm yr^{-1}) of Arabia–Eurasia convergence since 59 Ma. Moreover, our geodetic estimated rate is similar to the one estimated by McQuarrie *et al.* (2003) over the last 10 Myr. This may be an indication that the convergence rate given by NUVEL-1A is overestimated.

Fig. 7 represents the velocities in an Arabian reference frame defined with our Euler pole. The residual velocities of the sites east of the Arabian Plate in Israel and Jordan (GIL network, Wdowinski *et al.* 2001) show displacements. Sites located east of the Dead Sea Fault (DSF) (KATZ and ELRO) seem to belong to the Arabian Plate. This agrees well with the small amount of strain accumulation proposed by Pe'eri *et al.* (2002) in this region. Sites on the western part of the DSF move southward (KABR, BSHM, GILB, TELA, LHAV and RAMO) with an average velocity of 3 ± 3 mm yr^{-1}. This is consistent with geological (4 ± 2 mm yr^{-1}, Klinger *et al.* 2000a) and previous space geodetic studies (4 ± 1 mm yr^{-1}, Wdowinski *et al.* 2001). The low displacement of the site ELAT suggests a locked fault plane in this region, consistent with the stick-slip behaviour along this part of the DSF proposed by Klinger *et al.* (2000b).

3.2 Coherent motion of the central Iranian sites

Jackson & McKenzie (1984, 1988) suggested, mostly on the base of seismological observations, that the Central Iranian Block can be regarded as rigid (Fig. 2). If true, an Euler vector can describe displacements of such a rigid block. We estimated an Euler vector for the Central Iranian Block using five stations: ARDA, BIJA, HARA, MIAN and SHAH (Table 3, Fig. 2). The residual velocities for those five sites are inside the 1σ uncertainties. This indicates that the internal deformation is less than 2 mm yr^{-1}. This, together with the low level of earthquake occurrence (Fig. 2), suggests that the rigid description of the Central Iranian Block is appropriate since deviations from coherent behaviour are smaller than ∼10 per cent of the overall Arabia–Eurasia convergence.

Fig. 8 shows the velocity field in a reference frame fixed to the Central Iranian Block. The sites KERM, HAJI and TEHR do not

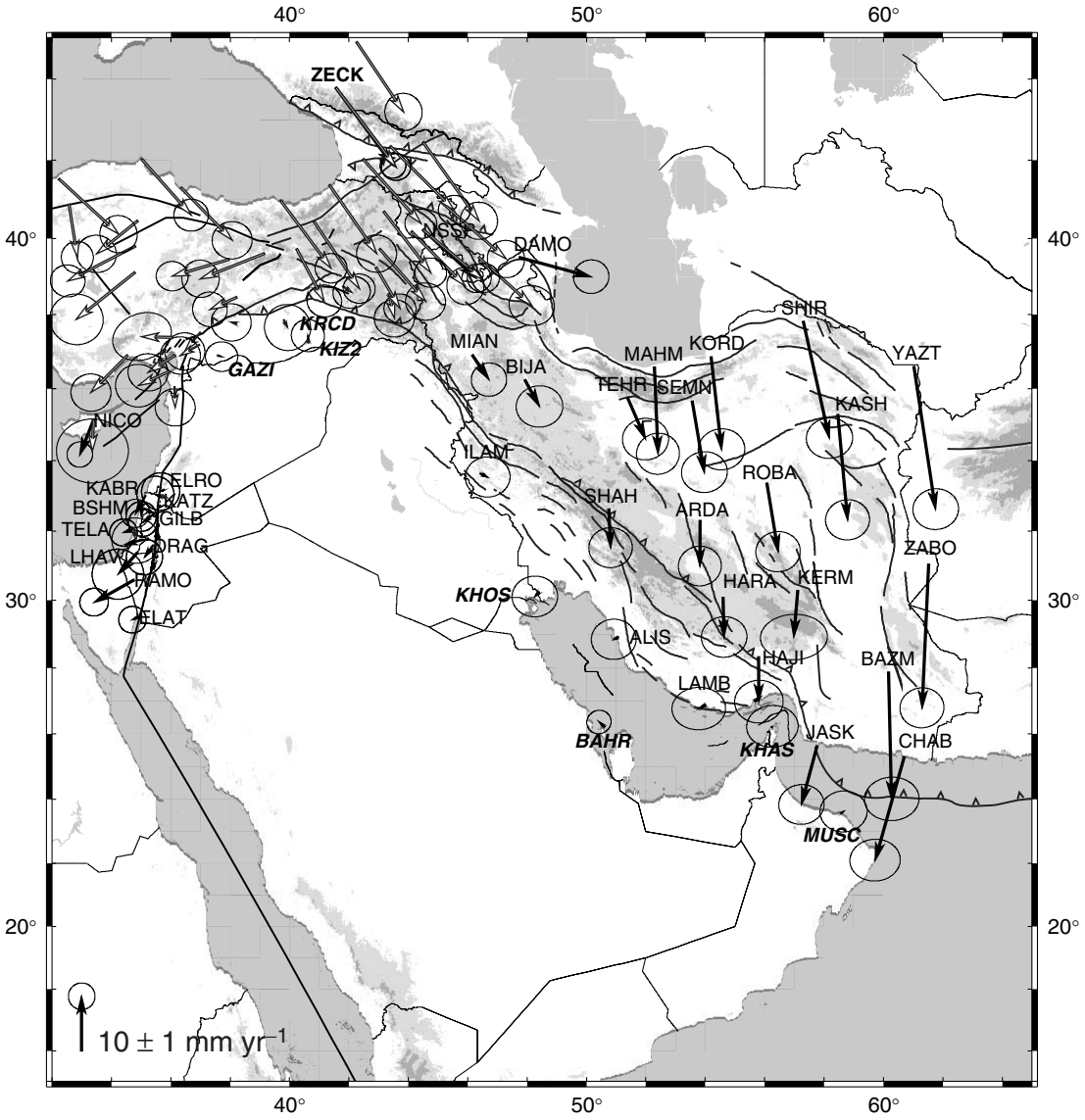

Figure 7. GPS horizontal velocities and their 95 per cent confidence ellipses in the Arabia-fixed reference frame for the period 1999–2001. Black vectors are from this study and black with white head from McClusky *et al.* (2000, 2003) studies. Tectonic symbols are the same as in Fig. 1.

move significantly relative to the Central Iranian Block. However, we did not include them to process the Euler vector of the Central Iranian Block with respect to Eurasia, because KERM and HAJI are not far from active seismic zones (Fig. 2) and TEHR is located north of the frontal thrusts bordering the southern side of the Alborz mountain belt. A perfectly coherent block motion of the site TEHR with the Central Iranian Block seems impossible since active thrust faults are described (e.g. De Martini *et al.* 1998; Berberian & Yeats 1999) south of Tehran. This could indicate that the thrust faults are locked and that no important elastic deformation occurred south of TEHR during the 2 yr of measurements (i.e. from 1999 September to 2001 October). A third survey may bring information on this point.

3.3 Arabia–Central Iranian Block convergence: the Zagros thrust and fold belt

The Zagros thrust and fold belt, as part of the Alpine–Himalayan mountain chain, extends for more than 1500 km in a NW–SE direction from eastern Turkey to the Minab–Zendan–Palami fault system in southern Iran (Haynes & McQuillan 1974; Stöcklin 1974; Blanc *et al.* 2003). This belt results from the closure of the Neo-Tethyan ocean due to a northeast-dipping subduction below the Iranian microcontinent. The subsequent collision beginning in the Neogene between the Arabian Plate and the Iranian Block (e.g. Stöcklin 1968; Falcon 1974; Berberian & King 1981; Berberian *et al.* 1982; Berberian 1983, 1995; Alavi 1994). This belt is underlined by an intense seismic activity (Fig. 2). The Main Zagros Thrust (MZT) also called the Main Zagros Reverse Fault underlines an abrupt cut-off of seismic activity (Berberian 1995; Maggi *et al.* 2000), and is commonly considered as the northern limit of the Arabian Plate because it marks the northeastern limit of the thick infra-Cambrian Hormuz Salt Formation (Stöcklin 1968; Berberian & King 1981).

Fig. 7 represents the velocity field in a reference frame fixed to the Arabian Plate. This reference frame allows estimation of the shortening in the Persian Gulf. It seems to be modest, since only 1 ± 2 mm yr^{-1} are accommodated between ALIS and LAMB relative to Arabia. Therefore, most of the convergence

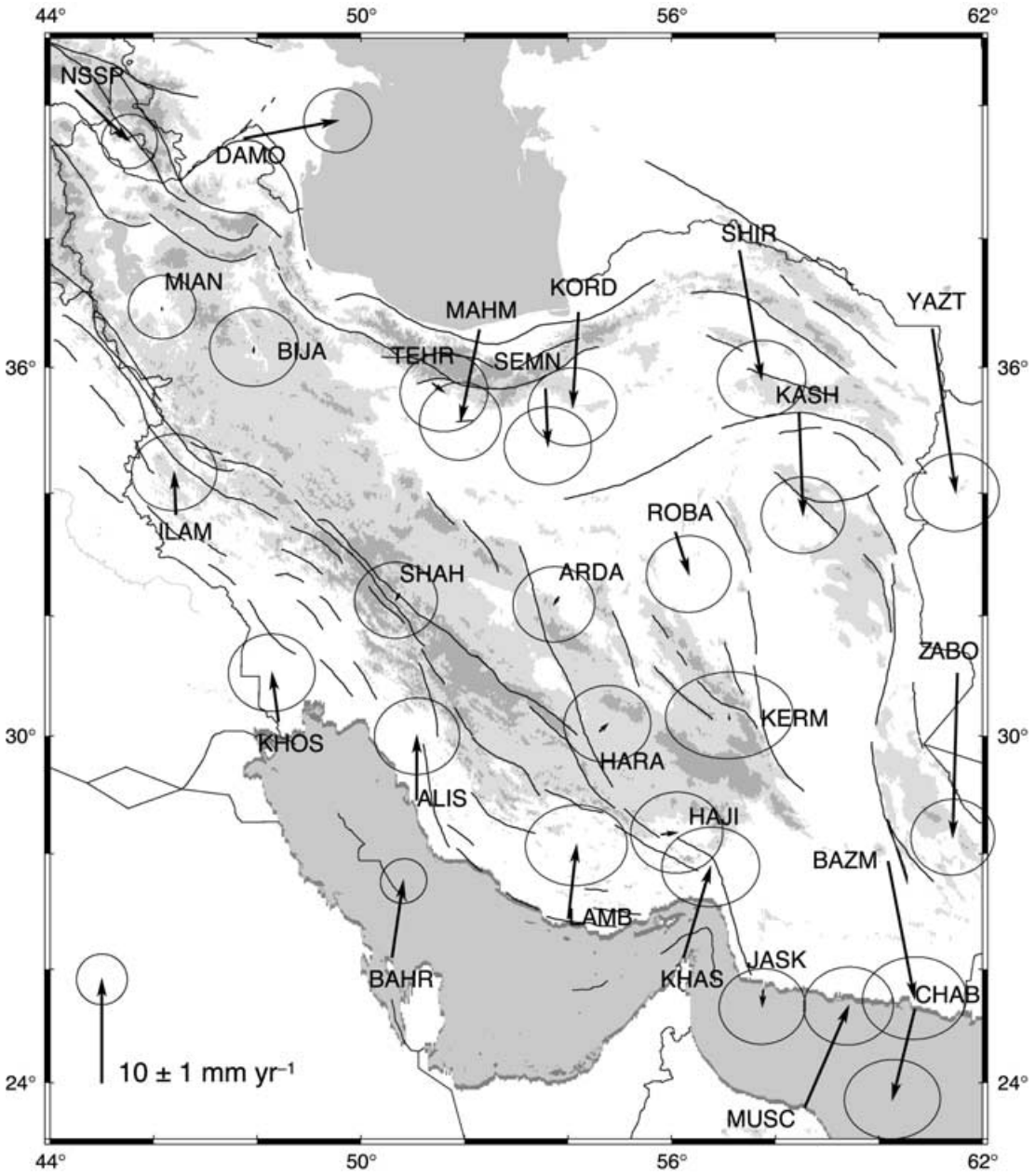

Figure 8. GPS horizontal velocities and their 95 per cent confidence ellipses in the central Iran-fixed reference frame for the period 1999–2001. Tectonic symbols are the same as in Fig. 1.

between Arabia and the Central Iranian Block is accommodated by the emerged part of the Zagros range as proposed by Berberian (1995).

To better assess the long-term convergence rate in the Zagros mountain belt, we used the velocity field in a reference frame fixed to the Central Iranian Block (Fig. 8). The main direction of shortening is roughly north–south, the orientations ranging from N7°E for LAMB to N3° W for ILAM. We observe a decreasing convergent rate from 9 ± 2 mm yr^{-1} in the southeastern Zagros (between KHAS and the Central Iranian Block) to 4.5 ± 2 mm yr^{-1} mm yr^{-1} in the northwestern part of the range (between KHOS and the Central Iranian Block). For the central Zagros the shortening rate is about 6.5 ± 2 mm yr^{-1} (between ALIS–LAMB and the Central Iranian Block). This rate is slightly smaller than the 10–15 mm yr^{-1} of north–south shortening proposed by Jackson *et al.* (1995). The discrepancy is partly induced by the boundary conditions of their model set up by the overestimated NUVEL-1A rate for the motion of the Arabian Plate. Our rate is reasonably consistent with the 10 ± 4 mm yr^{-1} roughly north–south suggested by Tatar *et al.* (2002). Assuming a constant shortening over the last 5 Myr, the total displacement is consistent with the geological estimations of Blanc *et al.* (2003) (i.e. 49 km over the last 5 Myr). By contrast, the 29 mm yr^{-1} of Holocene compression proposed by Mann & Vita-Finzi (1982) for the southeastern Zagros coastal plain are not consistent with our results.

The slip vector directions of the thrusting events show a fairly systematic angle of 35–40° to the east relative to the GPS vectors (Fig. 9). This and the focal mechanisms suggest a partition of the

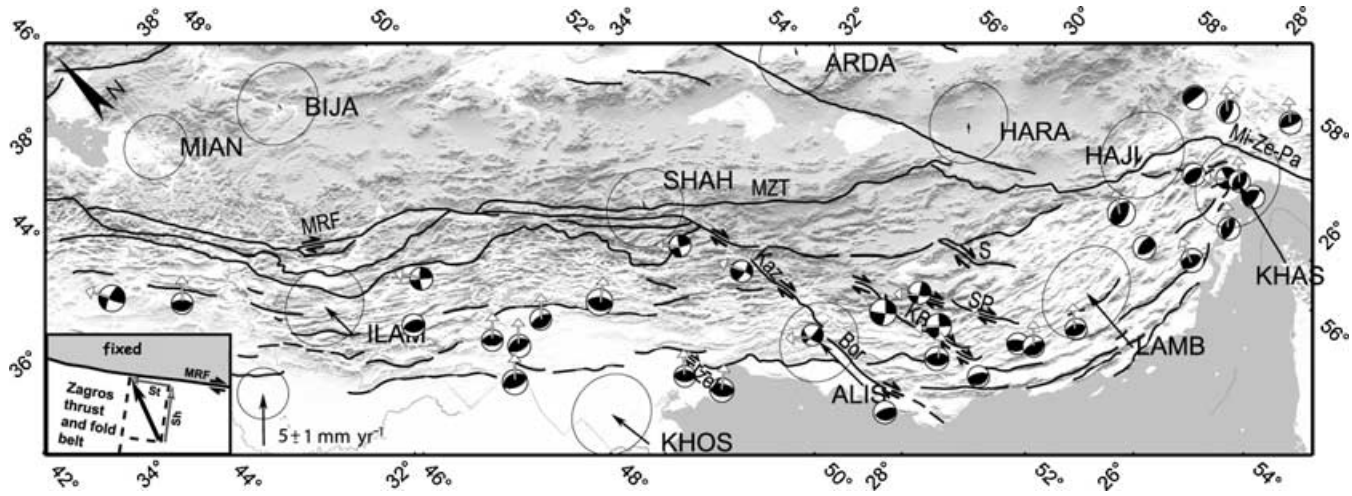

Figure 9. Map of the Zagros thrust and fold belt. Black arrows are the GPS horizontal velocities and their 95 per cent confidence ellipses in Central Iran-fixed reference frame. White arrows are the slip vectors given by Harvard; we plotted only those slip vectors when both slip vectors of the event gave the same direction. Focal mechanisms are from the Harvard catalogue (http://www.seismology.harvard.edu). Slip vectors indicate the motion of the southwest block. In the lower left corner, the pattern illustrates how the partitioning is estimated. St: strike-slip component, Sh: shortening component. MRF: Main Recent Fault, MZT: Main Zagros Thrust, Mi-Ze-Pa: Minab–Zendan–Palami fault zone, Kaz: Kazerun Fault, Bor: Borazjan Fault, KB: Kareh Bas Fault, SP: Sabz Pushan fault zone, S: Sarvestan Fault.

deformation between thrust and strike-slip structures in agreement with previous studies (e.g. Berberian 1995; Talebian & Jackson 2002). Several strike-slip faults are identified in the Zagros. One of the most important is the Main Recent Fault (MRF) (Fig. 9). This fault trends NW–SE and forms the northeastern border of the northern Zagros mountains (Tchalenko & Braud 1974). Evidence of large earthquakes lying on this fault (e.g. M_s 7.4 in 1909 and 6.7 in 1957) led several authors (e.g. Braud & Ricou 1975; Ricou *et al.* 1977; Jackson & McKenzie 1984; Jackson & McKenzie 1988; Jackson 1992; Talebian & Jackson 2002) to consider the MRF and the North Anatolian Fault (NAF) as an almost continuous active strike-slip zone on the northern Arabian and Anatolian plate margins (Fig. 1). Using geomorphic data, Talebian & Jackson (2002) have proposed a cumulated right-lateral displacement of ∼50 km. Assuming that the MRF and the NAF represent an almost continuous zone active since the Pliocene, they suggested a strike-slip rate of 10–17 mm yr^{-1}. In contrast, assuming that most of the strike-slip motion in this part of the range occurs on the MRF (inset of Fig. 9), and using the sites of ILAM and KHOS far from the fault in a reference frame fixed to the Central Iranian Block, we estimated a strike-slip rate on the MRF of 3 ± 2 mm yr^{-1}. This is dramatically low with respect to the previously proposed rates. Assuming that such a low constant strike-slip rate has been responsible for the 50 km observed by Talebian & Jackson (2002), the MRF could have started at any time in between 50 Ma and 10 Ma. Therefore, the MRF could have started at the beginning of the collision which seems to occur before 10 Ma (Hessami *et al.* 2001; McQuarrie *et al.* 2003). Using GPS measurements, McClusky *et al.* (2000) calculated a maximum right-lateral strike-slip rate of 24 ± 2 mm yr^{-1} along the NAF. Therefore, the MRF does not appear to be the eastern continuation of the NAF and a part of the right-lateral motion along the NAF may be accommodated elsewhere to the north (see below and Fig. 10) as proposed by Jackson (1992).

In the central and southern Zagros no partitioning is reported, the strike-slip faults are inside the fold and thrust belt and they are orientated NNW–SSE to N–S rather than NW–SE as the MRF (Sabz Pushan, Sarvestan, Kareh Bas, Kazerun Borazjan and Izeh, Fig. 9). Therefore estimating rates for these faults is impossible with our network pattern. However, the rates (∼14.5 mm yr^{-1}) proposed by Berberian (1995) for the Kazerun and Borazjan faults seem too high due to the lack of large differential motion between the southern Zagros margin sites of KHOS, ALIS and LAMB.

3.4 Southeastern Iran: Makran subduction and large lateral displacements

The Arabia–Eurasia convergence involves intracontinental shortening everywhere in Iran except its southern margin east of about 58°E, where the Oman Sea subducts northward under the Makran (Byrne *et al.* 1992). The remnant Tethys oceanic crust has been subducting since Cretaceous times with a low angle under southeastern Iran and the Helmand Block (Fig. 1). The deformation front follows approximately the 3000 m depth contours (White 1982; White & Louden 1982; Ravaut *et al.* 1997). A large amount of material has been accreted since it has enlarged the upper plate by more than 300 km toward the south.

Assuming a completely rigid plate motion DeMets *et al.* (1994) estimated the convergence rate between Arabia and Eurasia to be 36.5 mm yr^{-1} near the Strait of Hormuz and 42 mm yr^{-1} at the eastern boundary of the Makran. GPS results (Fig. 4) indicate lower velocities of 25 ± 2 mm yr^{-1} near the Strait of Hormuz (KHAS) and 27 ± 2 mm yr^{-1} in eastern Oman (MUSC). The shortening rates provided by the GPS for the Gulf of Oman range between 11 ± 2 mm yr^{-1} (JASK relative to Arabia) and 19.5 ± 2 mm yr^{-1} (CHAB relative to Arabia). The site of JASK is located near the Minab–Zendan–Palami NNW–SSE fault system (Fig. 1). This fault zone marks the transition between the Zagros collision and the Makran subduction. Therefore this site could be influenced by the collision. The shortening rate of 19.5 ± 2 mm yr^{-1} at N16°E ± 5° between CHAB and the Arabian Plate seems more representative of the subduction rate. Such high velocities should produce large earthquakes. However, the present-day seismicity level in the Makran is quite low. Most of the events are thought to be related to the bending within the

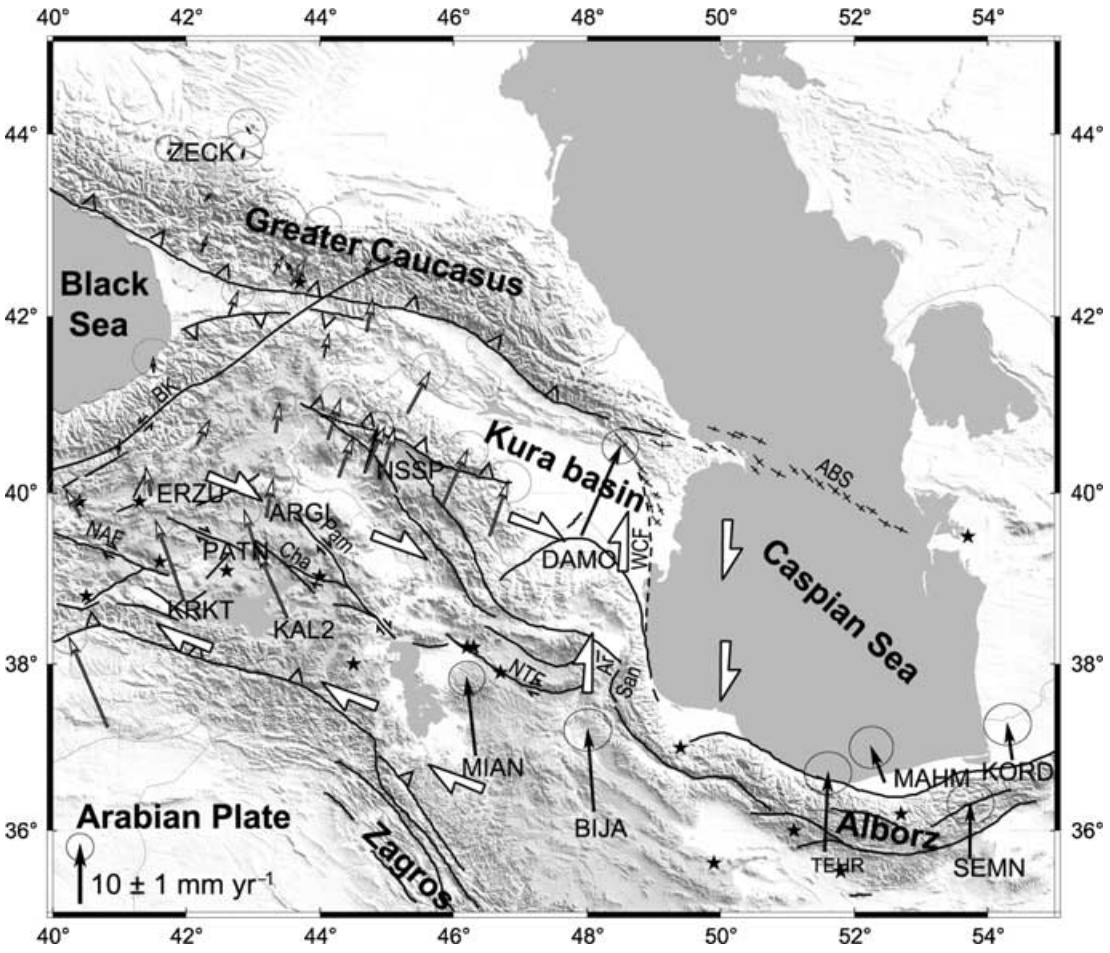

Figure 10. GPS horizontal velocities and their 95 per cent confidence ellipses (in the Eurasia-fixed reference frame) for the northwestern Iran, eastern Turkey and Caucasus area. Black vectors are from this study and black with white heads from the McClusky *et al.* (2000) study. The velocities for the NSSP station are quite similar. Right stepping *en echelon* fold axis are plotted near the WCF. ABS: Apsheron Balkan Sills, Ar: Ardebil Fault, BK: Borzhomi-Kazbeg, Cha: Chalderan, NAF: North Anatolian Fault, NTF: North Tabriz Fault, Pam: Pambuk, San: Sangavar Fault, WCF: West Caspian Fault. Historical seismicity ($M >$ 7) from the NEIC catalogue is indicated by black stars.

down-going plate at intermediate depths (Byrne *et al.* 1992). Events lying on the plate interface near the coast are known only east of the Sistan suture zone, where three large historical earthquakes occurred ($M_w > 7$). CHAB is located on the southeast Iranian coast, not far from the deformation front, and no large has earthquake occurred in this part since at least 1483 (Byrne *et al.* 1992). Assuming a locked interface since 1483, about 6–9 m of north–south shortening has occurred. This corresponds to a slip release of a $M_s \approx 8$ (Wells & Coppersmith 1994) earthquake such as the 1945 one ($M_w =$ 8.1) in eastern Makran. If we assume behaviours comparable to the sub-Andean subduction zone (Bevis *et al.* 2001) or the silent slip events of the Cascadia zone (Dragert *et al.* 2001), the geodetic rate of 19.5 $\pm$ 2 mm yr^{-1} could be different from the long-term value. Therefore, 19.5 $\pm$ 2 mm yr^{-1} could be a minimum value for the subduction rate; the maximum rate is the velocity of the Arabian margin of the Gulf of Oman relative to Eurasia (e.g. 27 $\pm$ 2 mm yr^{-1} for the site MUSC). Without regular GPS recording in the Makran, it is probably too early to qualify the western part as aseismic subduction.

The boundaries of the Makran wedge are quite complicated tectonic areas. A major transpressional strike-slip system forms the eastern boundary (Ornach-Nal and Chaman fault zones, Fig. 1). This system is accommodating left-lateral motion between the Indian Plate and the Makran and Helmand blocks, and has been responsible for several destructive earthquakes (Quittmeyer & Jacob 1979). On the other hand, the western boundary forms a transition zone between the Zagros continental collision and the Makran oceanic subduction (Haynes & McQuillan 1974; Stöcklin 1974; Falcon 1976; Kadinsky-Cade & Barazangi 1982), with a very low seismicity energy release. If no large rotation occurs in this zone, the right-lateral displacement between KHAS and JASK is about 11 $\pm$ 2 mm yr^{-1}. This rate is consistent with the motion deduced from tectonic observations in this area (Regard 2003).

The motion of sites located on the eastern Iranian border (i.e. YAZT and ZABO) suggests that the displacement rate of the Helmand Block is small relative to Eurasia. This agrees well with the proposition of Jackson & McKenzie (1984) who suggested that little deformation occurs east of 61°E due to the abrupt decrease of the seismicity pointed out by Gutenberg & Richter (1954). Moreover, this small displacement rate suggests right-lateral shear on both east and west sides of the Lut Block between the Central Iranian Block and the Helmand Block. The velocity of ZABO with respect to the Central Iranian Block (Fig. 9) is 16 $\pm$ 2 mm yr^{-1} to the south.

This involves a maximum amount of right-lateral strike-slip on both east and west sides of the Lut Block of about 16 mm yr^{-1}.

3.5 The South Caspian Basin and the surrounding mountain ranges

The South Caspian Basin is a relatively aseismic block involved in the collision zone between Eurasia and Arabia. This unusual thick 'basaltic' lower crust (15–18 km) is overlaid by a thick sedimentary sequence (15–20 km) (Mangino & Priestley 1998; Brunet *et al.* 2003). Several origins have been proposed for this remnant piece of oceanic floor: a part of a late Mesozoic or early Tertiary marginal basin (Berberian 1981, 1983; Zonenshain & Le Pichon 1986; Philip *et al.* 1989), a remnant part of the Tethys Ocean (Dercourt *et al.* 1986; Nadirov *et al.* 1997) or a pull-apart basin (Sengör 1990). The South Caspian Basin is expected to be relatively rigid. By contrast, deformation and uplift are concentrated in the surrounding mountain ranges (Axen *et al.* 2001; Jackson *et al.* 2002).

East of the South Caspian Basin, the Kopet-Dag is accommodating the deformation between the Turan to the north and the Lut–central Iran to the south. Only one site is located south of the Kopet-Dag range (KHAS). Therefore, it allows a quite rough estimation of the Kopet-Dag shortening rate of 6.5 $\pm$ 2 mm yr^{-1} at N11°E $\pm$ 5°. The site SHIR inside the range suggests a distributed deformation in the mountain belt. Due to the lack of GPS sites on the Turan Shield, we cannot estimate the long-term motion on the Ashkabad Fault. Assuming that the Turan Shield is part of stable Eurasia the right-lateral motion on the Ashkabad Fault using the site SHIR should be less than 1 mm yr^{-1}. Such rates are much lower than the15 mm yr^{-1} of north–south shortening (i.e. 75 km over the last 5 Myr, Lyberis & Manby 1999) and the 3–8 mm yr^{-1} of right-lateral displacements on the Ashkabad Fault (Trifonov 1978; Lyberis & Manby 1999).

GPS measurements suggest 8 $\pm$ 2 mm yr^{-1} of north–south shortening between the Central Iranian Block and the site on the southern Caspian shore (MAHM). Therefore, shortening in central Alborz seems to be 8 $\pm$ 2 mm yr^{-1}, in agreement with the geological rates of $\sim$5 mm yr^{-1} over the last 5 Ma (Allen *et al.* 2003a). However, the motion of the site TEHR coherent with the Central Iranian Block motion needs to be confirmed by new measurements since active faults are described south of this site (De Martini *et al.* 1998; Berberian & Yeats 1999). In eastern Alborz, 3.5 $\pm$ 2 mm yr^{-1} are accommodated between SEMN and KORD and 5 $\pm$ 2 mm yr^{-1} are accommodated between ARDA and SEMN. Despite the long distance between these two points, the deformation between ARDA and SEMN may occur on external thrust of eastern Alborz as suggested by historical events (Berberian & Yeats 1999). The whole compression in Alborz seems to be roughly orientated north–south with a rate of about 8 $\pm$ 2 mm yr^{-1}. The Arabian–Eurasian convergence is not accommodated only in the Zagros and Alborz, as rates of 6.5 $\pm$ 2 mm yr^{-1} at N15°W $\pm$ 10° (MAHM and KORD) occur on the southern Caspian shore. Therefore, the shortening rate absorbed by the Alborz mountain belt and the South Caspian Basin is about 14 $\pm$ 2 mm yr^{-1}. This is consistent with the $\sim$14 mm yr^{-1} based on the velocity triangle of Jackson *et al.* (2002) revised by Allen *et al.* (2003b) using the Arabia–Eurasia convergence rates of Sella *et al.* (2002).

In northwestern Iran, eastern Turkey and the Caucasus, our results agree with McClusky *et al.* (2000) for the permanent stations in Yerevan (NSSP) and Zelenchukskaya (ZECK) (Fig. 10). Moreover, the site in northern Talesh (DAMO) shows a direction coherent with the vectors of McClusky *et al.* (2000) in the vicinity of the Kura Basin. Large right-lateral displacements take place between DAMO and the Central Iranian Block (Figs 8 and 10). Our measurements suggest $\pm$ 2 mm yr^{-1} of right-lateral displacements for the entire set of faults between DAMO and BIJA. NW–SE faults in the Tabriz region, well known for its large historical seismicity (Berberian & Yeats 1999), appears as good candidates to accommodate the deformation. Moreover, the rate of 8 $\pm$ 2 mm yr^{-1} is consistent with the 5–8 mm yr^{-1} along the WNW–ESE right-lateral strike-slips in eastern Turkey indicated by the measurements of McClusky *et al.* (2000) (between KRKT–ERZU, ARGI–PATN or ARGI–KAL2, Fig. 10).

4 ADDITIONAL PRESENT-DAY KINEMATICS IN IRAN

Our GPS measurements in Iran provide the first-order present-day kinematics of Iran. Even if some areas of the network remain poorly constrained. Using other data (e.g. historical seismicity, geomorphic evidence) we try to estimate some rates in the region not well sampled by our network (i.e. northwestern Iran, the South Caspian Basin surroundings and eastern Iran).

GPS measurements suggest right-lateral displacements in northwestern Iran. The right-lateral deformation occurring between DAMO and the Central Iranian Block could be distributed along NW–SE Iranian and Armenian fault systems. Palaeoseismological studies (Philip *et al.* 2001) suggest low velocities and long recurrence time intervals (2.24 $\pm$ 0.96 mm yr^{-1}, 3000–4000 yr) along the Armenian faults. The recurrence time intervals on the North Tabriz Fault (NTF) are shorter ($\sim$250 yr, Berberian & Yeats 1999), with large events up to $M = 7.7$. If we assume that about 5 mm yr^{-1} of right-lateral displacement occurs along the NTF with a recurrence time interval of 250 yr, the average displacement is about 1.25 m for each event. Using an empirical relationship between moment magnitude and maximum displacement, the magnitude is $M \approx 7$ (Wells & Coppersmith 1994). This agrees with the magnitudes proposed by Berberian & Yeats (1999) for the historical events along the NTF. Therefore, most of the right-lateral displacements could be located on the NTF and other faults in northwestern Iran (Pambukh, Chalderan and Badalan, Fig. 10). This fault bundle could be the eastward prolongation of the North Anatolian Fault.

Around the South Caspian Block, the high velocities in the Eurasian reference frame of DAMO and BIJA in comparison with the velocities of MAHM and KORD suggest strike-slip motion west of the Caspian Sea. This right-lateral displacement could be located east of the Kura Basin on the West Caspian Fault (WCF) as suggested by several authors. Right-lateral displacements are pointed out by Berberian & Yeats (1999) along the Sangavar and Ardebil faults (Fig. 10). Right-stepping *en echelon* folds and NW–SE right-lateral strike-slip faults have been described by Trifonov (1978) and Kopp (1982, 1997) away from the thrusts west of Baku and entering the Kura Basin. Based on this evidence of transpression associated to an apparent offset of the Kura River Karakhanian *et al.* (1997) and Nadirov *et al.* (1997) drew the WCF as a north–south strike-slip fault from the southeastern Caucasus to the Talesh (Fig. 10). Other authors (Allen *et al.* 2003b) suggested that north–south right-lateral strike-slip motion exists only in the Talesh (Sangavar Fault). To do so, they assume clockwise rotation of crustal blocks in the Talesh. Our GPS network was not designed to answer such a question. However, the orientation of the vector for the site DAMO is consistent with those of Armenian sites (McClusky *et al.* 2000) and no active strike-slip faulting is reported between these two regions (Allen *et al.* 2003b). Therefore, it seems that if a local rotation of a block

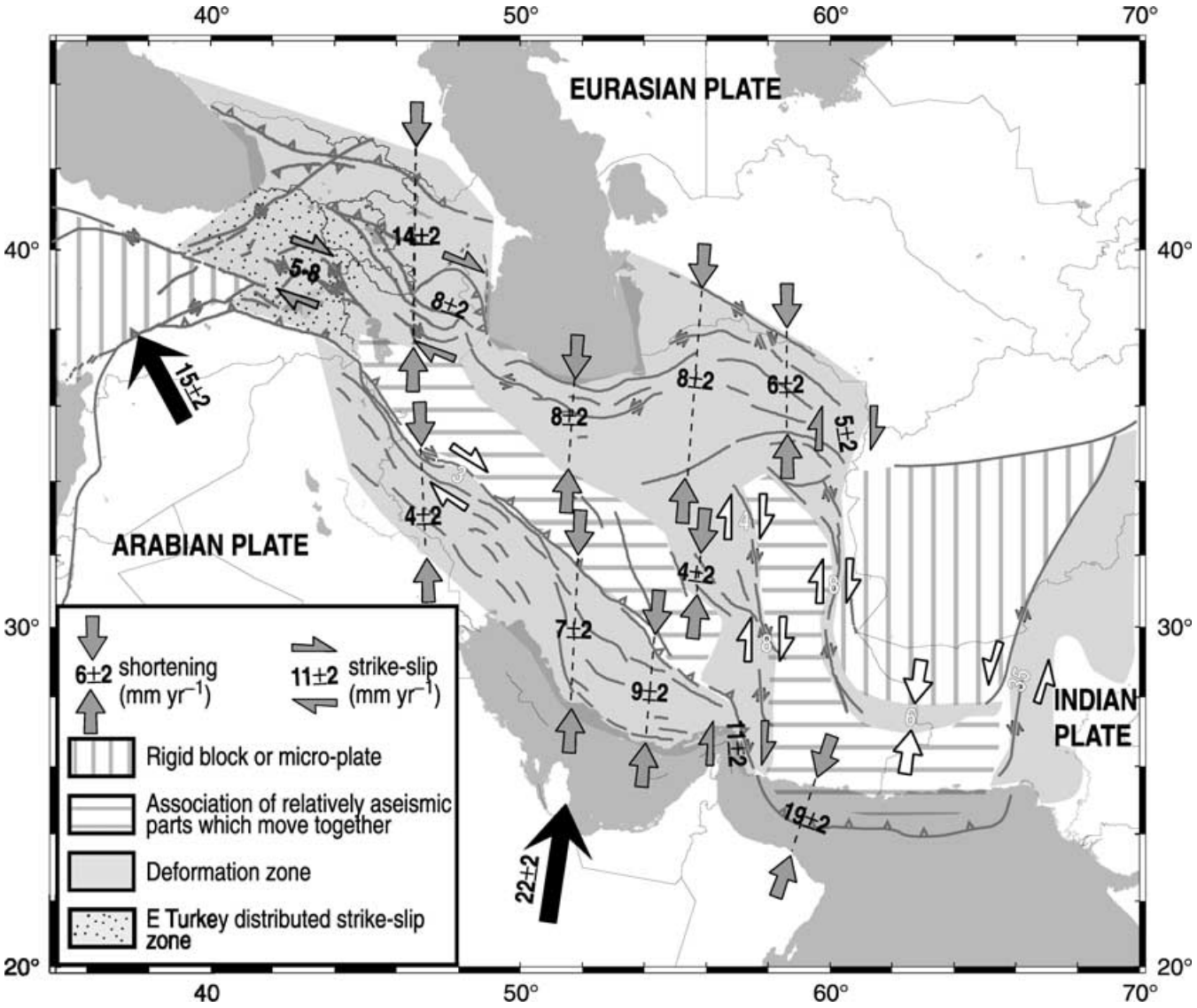

Figure 11. Schematic illustration of the main results of this study. Hatching shows areas of coherent motion, grey zones are actual deformation areas (see legend). Heavy arrows in black indicate the actual motion of the Arabian plate relative to the Eurasia. Grey arrows are deformation rates directly measured with GPS. Rates in eastern Turkey are deduced from McClusky *et al.* (2000). White arrows are deduced rates from GPS, geological evidence and seismology, for motion along the Chaman Fault and the associated deformation zone the velocity is deduced from the REVEL model (Sella *et al.* 2002). All the rates are given in mm yr^{-1}.

exists in the area of DAMO, its magnitude is too low to explain the GPS velocity differences between the South Caspian Basin and the northern Talesh. Assuming that all the southern Caspian shore is moving at 6 mm yr^{-1} to the north, the right-lateral strike-slip rate along the WCF would be about 7–8 mm yr^{-1}. However, we emphasize that this rate suffers from a large uncertainty.

The western and eastern borders of the Lut Block are described as large right-lateral strike-slip faults (e.g. Freund 1970; Mohajer-Ashjai *et al.* 1975; Kluyver *et al.* 1978; Camp & Griffis 1982; Tirrul *et al.* 1983; Berberian & Yeats 1999; Walker & Jackson 2002). A dextral shear of 16 ± 2 mm yr^{-1} occurs between ZABO and the Central Iranian Block. Because we have no site on the Lut Block, the displacements on the eastern and western Lut borders could not be measured directly. Conrad *et al.* (1982) suggested, using palaeomagnetic data, that no significant rotation occurs during the Plio-Quaternary for the Lut Block. Therefore the velocity orientation of the Lut should be consistent with the surrounding orientations (Central Iran, Makran, Kopet-Dag and Helmand). The right-lateral strike-slip motions reported along the north–south borders of the Lut imply that the north component of the velocity in the Lut is less than the ROBA velocity (12 ± 2 mm yr^{-1}). Because evidence of shortening is reported by Berberian & Yeats (1999) north of the Lut, the velocity of this block is greater than the KASH velocity (6.5 ± 2 mm yr^{-1}). On these bases, the velocity of the Lut relative to Eurasia should range between 6.5 and 12 mm yr^{-1}. BAZM velocity does not confirm this rate, but the site could be in the elastic deformation zone of a Sistan locked fault. Using an average value of 9 mm yr^{-1} for the Lut, the right-lateral strike-slip rates along the Lut border are about ∼9 mm yr^{-1} to the east, ∼7 mm yr^{-1} along the southwestern border and ∼3 mm yr^{-1} in the northwest (Fig. 11). However, we emphasize that these rates suffer from large uncertainties. The ∼3 mm yr^{-1} along the northwestern Lut border is consistent with the

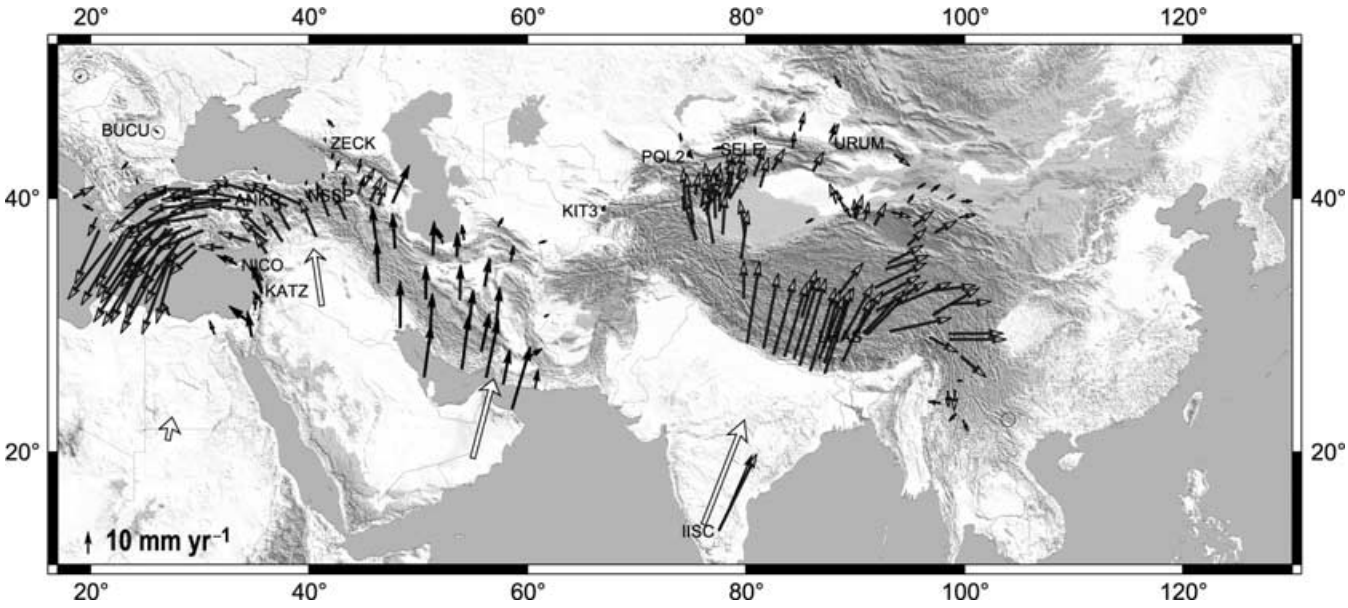

Figure 12. GPS horizontal velocities (in Eurasia-fixed reference frame) for the eastern Alpine–Himalayan belt. To avoid clutter, confidence ellipses and some sites have been removed. Black arrows are from this study, grey from McClusky *et al.* (2000) (blue in the online version) for the Anatolian region and from Wang *et al.* (2001) (red in the online version) for eastern Asia. White arrows are NUVEL-1A velocities.

$\sim$2 mm yr^{-1} suggested by Walker & Jackson (2002) for the Nayband Fault (Fig. 1). They extrapolated their rate to the Gowk Fault. GPS results do not support such extrapolation since 4 $\pm$ 2 mm yr^{-1} of N–S shortening occur in the region of the Kuh Banan and Lakarkuh faults (Fig. 8).

The rate of $\sim$9 mm yr^{-1} for the Lut Block relative to Eurasia is consistent with the 8 $\pm$ 2 mm yr^{-1} of the site CHAB. These velocities, the reverse fault tectonics in the Makran, the surroundings of the Jaz Murian depression pointed out by Berberian (1981), and the east–west continuous structures without north–south offset in the Makran (Byrne *et al.* 1992) suggest a coherent motion between the Lut and the Makran (Fig. 11). The eastern and western borders of the Makran accommodate transpressive constrain explaining the curvature of the Makran structures and the high velocity of JASK which is in the vicinity of the Minab–Zendan–Palami fault zone.

Taking together GPS and geological information, we summarize the schematic kinematic pattern of the present-day Arabia–Eurasia convergence zone in Iran (Fig. 11).

5 CONCLUSIONS

The GPS measurements of 1999–2001 in Iran and northern Oman provide new velocity data to quantify the present-day plate motions in the Middle East (Fig. 11). GPS velocities along the northeastern boundary of the Arabian Plate relative to Eurasia are systematically smaller than the NUVEL-1A estimations (about 10 mm yr^{-1} less). This corresponds to an Arabia–Eurasia Euler vector consistent with the results of Sella *et al.* (2002), Kreemer *et al.* (2003) and McClusky *et al.* (2003). Sites on the Central Iranian Block move in a coherent fashion, as predicted by Jackson & McKenzie (1984), with internal deformation smaller than 2 mm yr^{-1}. In the western part of the country, distributed deformation occurs among several fold and thrust belts. Between the Central Iranian Block and the Arabian Plate, the central Zagros accommodates about 7 $\pm$ 2 mm yr^{-1} of north–south shortening. The shortening rate decreases in northern Zagros, implying a right-lateral strike-slip rate along the Main Recent Fault of 3 $\pm$ 2 mm yr^{-1}, much smaller than geological estimates. North of the Central Iranian Block, the Alborz mountain range accommodates 8 $\pm$ 2 mm yr^{-1} of north–south compression. Sites along the southern Caspian shore indicate roughly northward motion at 6.5 $\pm$ 2 mm yr^{-1} relative to Eurasia. Therefore, the shortening rate accommodated by the Alborz and Caspian regions is consistent with that estimated by Jackson *et al.* (2002). In northwestern Iran large right-lateral motions are expected along the NW–SE Tabriz fault system and along a north–south fault bordering the western Caspian coast. Due to the low displacements on the Main Recent Fault, the right-lateral prolongation of the NAF could be in northwestern Iran (Fig. 11) rather than in northwestern Zagros as suggested by Jackson (1992). Most of the Arabia–Eurasia convergence rate west of the Caspian Sea seems to take place in the Caucasus and the Kura Basin. The tectonics of eastern Iran is mostly concentrated within the Makran subduction since the oceanic crust is subducting at 19.5 $\pm$ 2 mm yr^{-1} roughly north–south under the Makran Wedge. Therefore only 6.5 $\pm$ 2 mm yr^{-1} takes place in the Kopet-Dag north of the Lut Block, this is half of the rate based on geological evidence ($\sim$15 mm yr^{-1}, Lyberis & Manby 1999). The low velocity of sites east of 61°E suggests that displacement of the Helmand Block is very low relative to Eurasia. This implies that right-lateral displacements on the western and eastern borders of the Lut may be as large as 10 mm yr^{-1}.

Associated with other previous GPS results, our results bring a broad scale picture to the present-day kinematics of the Alpine–Himalayan mountain belt (Fig. 12). Hence, a large part of the convergence zone is covered by GPS measurements crossing eastern Turkey (e.g. McClusky *et al.* 2000), the Middle East (Nilforoushan *et al.*, 2003 and this study) and Asia (e.g. Wang *et al.* 2001). The main direction of convergence for this part of the Alpine–Himalayan mountain belt (from 40°E to 90°E of longitude) is roughly north–south (i.e. Arabia versus Eurasia and India versus Eurasia). However, we observe several types of continental deformation. To the west, in Turkey, the deformation is characterized by the lateral escape of

the Anatolian Plate with a block model behaviour (McClusky *et al.* 2000; Meade *et al.* 2002). In eastern Turkey, the Arabia–Eurasia convergence seems to be partitioned as proposed by Jackson (1992) between the convergence zone of the Caucasus to the north and the eastern Turkey distributed strike-slip zone to the south (McClusky *et al.* 2000). In northwestern Iran, the right-lateral motion seems to be localized on the North Tabriz fault system, which appears to be a potential eastward prolongation of the NAF. The western part of Iran shows distributed deformation among several mountains belts separated by the Central Iranian Block. The deformation in the eastern part of Iran is mostly accommodated by the Makran subduction. North of this subduction zone, there is a low level of deformation in the Makran and the Lut Block. This implies a stronger rigidity of this region, or a low oceanic–continental coupling avoiding an important transmission of the forces by the subduction to the upper plate. In comparison, in western Iran, the continent–continent coupling probably allows a larger coupling force. The Helmand Block seems to belong to the Eurasian Plate as proposed by Jackson & McKenzie (1984), and the Chaman Fault accommodates the differential motion between India and the Helmand Block. The deformation of the eastern part of the Alpine–Himalayan mountain belt seems to be distributed between broad deformation zones (e.g. the Tibetan Plateau and Tian Shan, Wang *et al.* 2001) and rigid block motion (e.g. the Tarim Basin, Shen *et al.* 2001). At the eastern end of the arc we observe lateral escape (e.g. the Sagaing Fault, Vigny *et al.* 2003). Therefore, one may note that the activity of large strike-slip faults of this part of the Alpine–Himalayan mountain belt (e.g. NAF, Minab–Zendan–Palami fault system, Chaman Fault and Sagaing Fault) results from the velocity differential due to the juxtaposition of two kinds of coupling (ocean–continent and continent–continent).

ACKNOWLEDGMENTS

We would like to thank all the participants in the GPS measurements who helped during the fieldwork to make these experiments successful. This project was sponsored by the French CNRS-INSU 'Intérieur de la Terre' programme, the National Cartographic Center (NCC-Tehran), the International Institute of Earthquake Engineering and Seismology (IIEES-Tehran) and the French Embassy in Iran. The CNRS-INSU and NCC provided the GPS receivers. We thank J. F. Ritz and H. Philip for many helpful geological discussions and R. W. King for his good advices on GAMIT-GLOBK software. We also thank Mikhail Kogan who provided us with a program to compute the Euler vectors. This paper benefited from constructive reviews of Eric J.-P. Blanc, Mark Allen and an anonymous reviewer. The maps in this paper were produced using the public domain Generic Mapping Tools (GMT) software (Wessel & Smith 1995).

REFERENCES

Alavi, M., 1994. Tectonics of the Zagros orogenic belt of Iran: new data and interpretation, *Tectonophysics,* **229,** 211–238.

Allen, M., Ghassemi, M.R. Sharabi, M. & Qorashi, M., 2003a. Accommodation of late Cenozoic oblique shortening in the Alborz range, Iran, *J. Struct. Geol.,* **25,** 659–672.

Allen, M.B., Vincent, S.J., Alsop, I., Ismail-zadeh, A. & Flecker, R., 2003b. Late Cenozoic deformation in the South Caspian region: effects of a rigid basement block within a collision zone, *Tectonophysics,* **366,** 223–239.

Altamimi, Z., Sillard, P. & Boucher, C., 2002. ITRF2000: a new release of the International Terrestrial Reference Frame for earth sciences applications, *J. geophys. Res.,* **107**(B10), NIL_119–NIL_137.

Ambraseys, N.N. & Melville, C.P., 1982. *A History of Persian Earthquakes*, Cambridge University Press, New York.

Axen, G.J., Lam, P.S., Grove, M. & Stockli, D.F., 2001. Exhumation of the west-central Alborz mountains, Iran, Caspian subsidence, and collision-related tectonics, *Geology,* **6,** 559–562.

Berberian, F., Muir, I.D., Pankhurst, R.J. & Berberian, M., 1982. Late Cretaceous and early Miocene Andean-type plutonic activity in northern Makran and Central Iran, *J. geol. Soc. Lond.,* **139**(5), 605–614.

Berberian, M., 1981. Active faulting and tectonics of Iran, in *Zagros-Hindu Kush-Himalaya Geodynamic Evolution*, American Geophysical Union Geodynamic Series, Vol. 3, pp. 33–69, ed. Gupta, H.K., and Delany, F.M. American Geophysical Union, Washington, DC.

Berberian, M., 1983. The southern Caspian: a compressional depression floored by a trapped, modified oceanic crust, *Can. J. Earth Sci.,* **20**(2), 163–183.

Berberian, M., 1995. Master 'blind' thrust faults hidden under the Zagros folds: active basement tectonics and surface morphotectonics, *Tectonophysics,* **241,** 193–224.

Berberian, M. & King, G.C.P., 1981. Towards a paleogeography and tectonic evolution of Iran, *Can. J. Earth Sci.,* **18**(2), 210–285.

Berberian, M. & Yeats, R.S., 1999. Patterns of historical earthquake rupture in the Iranian Plateau, *Bull. seism. Soc. Am.,* **89,** 120–139.

Beutler, G., Morgan, P. & Neilan, R., 1993. Geodynamics: tracking satellites to monitor global change, *GPS World,* **4,** 40–46.

Bevis, M., Kendrick, E., Smalley, R., Brooks, B., Allmendinger, R. & Isacks, B., 2001. On the strength of interplate coupling and the rate of back arc convergence in the central Andes: an analysis of the interseismic velocity field, *Geochem. Geophys. Geosys.,* **2**, (2001GC000198).

Blanc, E.J.-P., Allen, M.B., Inger, S. & Hassani, H., 2003. Structural styles in the Zagros Simple Folded Zone, Iran, *J. Geol. Soc. Lond.,* **160,** 401–412.

Bock, Y., Behr, J., Fang, P., Dean, J. & Leigh, R., 1997. Scripps Orbit and Permanent Array Center (SOPAC) and Southern Californian Permanent GPS Geodetic Array (PGGA), in *The Global Positioning System for the Geosciences*, pp. 55–61, National Academy Press, Washington, DC.

Braud, J. & Ricou, L.E., 1975. Eléments de continuité entre le Zagros et la Turquie du Sud-Est, *Bull. Soc. Geol. Fr.,* **7,** 1015–1023.

Brunet, M.-F., Korotaev, M.V., Ershov, A.V. & Nikishin, A.M., 2003. The south Caspian basin: a review of its evolution from subsidence modelling, *Sedim. Geol.,* **156,** 119–148.

Byrne, D.E., Sykes, L.R. & Davis, D.M., 1992. Great thrust earthquakes and aseismic slip along the plate boundary of the Makran subduction zone, *J. geophys. Res.,* **97,** 449–478.

Camp, V.E. & Griffis, R.J., 1982. Character, genesis and tectonic setting of igneous rocks in the Sistan suture zone, eastern Iran, *Lithos,* **15,** 221–239.

Chu, D. & Gordon, G., 1998. Current plate motions across the Red Sea, *Geophys. J. Int.,* **135,** 313–328.

Conrad, G., Montigny, R., Thuizat, R. & Westphal, M., 1982. Dynamique cénozoïque du bloc du Lout (Iran) d'après les données paléomagnétiques, isotopiques, pétrologiques et structurales, *Géol. Méditerranéenne,* **9**(1), 23–32.

De Martini, P.M., Hessami, K., Pantosti, D., D'Addezio, G., Alinaghi, H. & Ghafori-Ashtiany, M., 1998. A geologic contribution to the evaluation of the seismic potential of the Kahrizac fault (Tehran, Iran), *Tectonophysics,* **287,** 187–199.

DeMets, C., Gordon, R.G., Argus, D.F. & Stein, S., 1990. Current plate motions, *Geophys. J. Int.,* **101,** 425–478.

DeMets, C., Gordon, R.G., Argus, D.F. & Stein, S., 1994. Effects of recent revisions to the geomagnetic reversal time scale on estimates of current plate motions, *Geophys. Res. Lett.,* **21,** 2191–2194.

Dercourt, J. *et al.,* 1986. Geological evolution of the Tethys belt from the Atlantic to the Pamirs since the Lias, *Tectonophysics,* **123,** 241–315.

Dong, D., Herring, T.A. & King, R.W., 1998. Estimating regional deformation from a combination of space and terrestrial geodetic data, *J. Geodyn.,* **72,** 200–211.

Dragert, H., Wang, K. & James, T.S., 2001. A silent slip event on the deeper Cascadia subduction interface, *Science,* **292,** 1525–1528.

Engdahl, R., van der Hilst, R. & Buland, R., 1998. Global teleseismic earthquake relocation with improved travel times and procedures for depth determination, *Bull. seism. Soc. Am.,* **88,** 722–743.

Falcon, N.L., 1974. Southern Iran: Zagros Mountains, in *Mesozoic-Cenozoic Orogenic Belts, Data for Orogenic Studies*, pp. 199–211, ed. Spencer, A. M., Geological Society of London Special Publication.

Falcon, N.L., 1976. The Minab Anticline: the Geological Evolution of Southern Iran: the report of the Iranian Makran expedition, *Geographical J.,* **142,** 409–410.

Feigl, K.L. *et al.*, 1993. Space geodetic measurement of crustal deformation in central and southern California, *J. geophys. Res.,* **98,** 21 677–21 712.

Freund, R., 1970. Rotation of strike slip faults in Sistan, southeast Iran, *J. Geol.,* **78,** 188–200.

Gutenberg, B. & Richter, C.F., 1954. *Seismicity of the Earth and Associated Phenomena*, Princeton University Press, Princeton, New Jersey.

Haynes, S.J. & McQuillan, H., 1974. Evolution of the Zagros suture zone, southern Iran, *Bull. geol. Soc. Am.,* **85,** 739–744.

Herring, T.A., 2002. *GLOBK: Global Kalman Filter VLBI and GPS Analysis Program*, version 10.0, Massachusetts Institute of Technology, Cambridge, MA.

Hessami, K., Koyi, H.A., Talbot, C.J., Tabassi, H. & Shabanian, E., 2001. Progressive unconformities within an evolving foreland fold-thrust belt, Zagros Mountains, *J. geol. Soc. Lond.,* **158,** 969–981.

Jackson, J.A., 1992. Partitioning of strike-slip and convergent motion between Eurasia and Arabia in eastern Turkey and Caucasus, *J. geophys. Res.,* **97,** 12 471–12 479.

Jackson, J.A. & McKenzie, D.P., 1984. Active tectonics of the Alpine-Himalayan Belt between western Turkey and Pakistan, *Geophys. J. R. astr. Soc.,* **77,** 185–246.

Jackson, J.A. & McKenzie, D.P., 1988. The relationship between plate motions and seismic tensors, and the rates of active deformation in the Mediterranean and Middle East, *Geophys. J. R. astr. Soc.,* **93,** 45–73.

Jackson, J.A., Haines, J. & Holt, W., 1995. The accommodation of the Arabia-Eurasia plate convergence in Iran, *J. geophys. Res.,* **100,** 15 205–15 219.

Jackson, J.A., Priestley, K., Allen, M. & Berberian, M., 2002. Active tectonics of the South Caspian Basin, *Geophys. J. Int.,* **148,** 214–245.

Kadinsky-Cade, K. & Barazangi, M., 1982. Seismotectonics of southern Iran : the Oman Line, *Tectonics,* **1,** 389–412.

Karakhanian, A.S., Djrbashian, R.T., Trifonov, V.G., Philip, H. & Ritz, J.F., 1997. Active faults and strong earthquakes of the Armenian upland, in *Historical and Prehistorical Earthquakes in the Caucasus*, pp. 181–187, eds Giardini, D. & Balassanian, S., Kluwer Academic, Dordrecht.

King, R.W. & Bock, Y., 2002. *Documentation for the GAMIT Analysis Software*, release 10.0, Massachusetts Institute of Technology, Cambridge, MA.

Klinger, Y., Avouac, J.-P., Abou Karaki, N., Dorbath, L., Bourles, D. & Reyss, J.L., 2000a. Slip rate on the Dead Sea transform fault in northern Araba valley (Jordan), *Geophys. J. Int.,* **142**(3), 755–768.

Klinger, Y., Avouac, J.-P., Dorbath, L., Abou Karaki, N. & Tisnerat, N., 2000b. Seismic behaviour of the Dead Sea fault along Araba valley, Jordan, *Geophys. J. Int.,* **142**(3), 769–782.

Kluyver, M., Griffis, R.J. & Tirrul, R., 1978. *Geology of the Lakar Kuh Quadrangle, 1:250,000, with Explanatory Report*, Geological Survey of Iran, Tehran, Iran.

Kopp, M.L., 1982. Nekotoryye voprosy pozdneal'piyskoy geodinamiki Yugo-Vostochnogo Kavkaza, Talysha i Nizhnekurinskoy vpadiny [Some problems of late Alpine geodynamics in the southeastern Caucasus, Talysh Mountains, and lower Kura Basin], in *Problemy Geodinamiki Kavkaza [Problems of Geodynamics in the Caucasus]*, pp. 99–105, eds Muratov, M.V.A., Sh, A., Belov, A.A., Khain, V.Ye. & Kuloshvili, S.I., Nauka, Moscow.

Kopp, M.L., 1997. *Lateral Escape Structures in the Alpine-Himalayan Collision Belt*, Russian Academy of Sciences, Geological Institute Transactions, Moscow.

Kreemer, C., Haines, A.J., Holt, W.E., Blewitt, G. & Lavallée, D., 2000. On the determination of a global strain rate model, *Earth planet. Sci. Lett.,* **52,** 765–770.

Kreemer, C., Holt, W.E. & Haines, A.J., 2003. An integrated global model of present-day plate motions and plate boundary deformation, *Geophys. J. Int.,* **154,** 8–34.

Langbein, J. & Johnson, H., 1997. Correlated errors in geodetic time series: implications for time-dependent deformation, *J. geophys. Res.,* **102,** 591–603.

Larson, K.M. & Agnew, D.C., 1991. Application of the Global Positioning to crustal deformation measurement: 1. Precision and accuracy, *J. geophys. Res.,* **96,** 16 547–16 565.

Lyberis, N. & Manby, G., 1999. Oblique to orthogonal convergence across the Turan block in the post-Miocene, *Am. Assoc. Petrol. Geol. Bull.,* **83,** 1135–1160.

Maggi, A., Jackson, J.A., Priestley, K. & Baker, C., 2000. A re-assessment of focal depth distribution in southern Iran, the Tien Shan and northern India: do earthquakes really occur in the continental mantle?, *Geophys. J. Int.,* **143,** 629–661.

Mangino, S. & Priestley, K., 1998. The crustal structure of the southern Caspian region, *Geophys. J. Int.,* **133,** 630–648.

Mann, C.D. & Vita-Finzi, C., 1982. Curve interpolation and folded strata, *Tectonophysics,* **88,** T7–T15.

Mao, A., Harrison, C. & Dixon, T., 1999. Noise in GPS coordinate time series, *J. geophys. Res.,* **104,** 2797–2816.

McClusky, S. *et al.*, 2000. GPS constraints on plate motions and deformations in eastern Mediterranean and Caucasus, *J. geophys. Res.,* **105,** 5695–5719.

McClusky, S., Reilinger, R., Mahmoud, S., Ben Sari, D. & Tealeb, A., 2003. GPS constraints on Africa (Nubia) and Arabia plate motions, *Geophys. J. Int.*, **155,** 126–138.

McQuarrie, N., Stock, J.M., Verdel, C. & Wernicke, B.P., 2003. Cenozoic evolution of Neotethys and implications for the causes of plate motions, *Geophys. Res. Lett.,* **30**(20), doi:10.1029/2003GL017992.

Mohajer-Ashjai, A., Behzadi, H. & Berberian, M., 1975. Reflections on the rigidity of the Lut block and recent crustal deformation in eastern Iran, *Tectonophysics,* **28,** 281–301.

Nadirov, R.S., Bagirov, E., Tagiyev, M. & Lerche, I., 1997. Flexural plate subsidence, sedimentation rates, and structural development of the superdeep South Caspian Basin, *Marine Petrol. Geol.,* **14,** 383–400.

Nilforoushan, F. *et al.*, 2003. GPS networks monitors the Arabia-Eurasia collision deformation in Iran, *J. Geodyn.*, **77,** 411–422.

Nowroozi, A.A. & Mohajer-Ashjai, A., 1985. Fault movements and tectonics of the eastern Iran: boundaries of the Lut plate, *Geophys. J. R. astr. Soc.,* **83,** 215–237.

Oral, B., 1994. Global Positioning System (GPS) measurements in Turkey (1988–1992): kinematics of the Africa-Arabia-Eurasia Plate collision zone, PhD Thesis, Massachusetts Institute of Technology, Cambridge, MA.

Pe'eri, S., Wdowinski, S., Shtibelman, A., Bechor, N., Bock, Y., Nikolaidis, R. & van Domselaar, M., 2002. Current plate motion across the Dead Sea Fault from three years of continuous GPS monitoring, *Geophys. Res. Lett.,* **29**(14), 42–1, 42–4.

Philip, H., Cisternas, A., Gvishiani, A. & Gorshkov, A., 1989. The Caucasus: an actual example of the initial stages of continental collision, *Tectonophysics,* **161,** 1–21.

Philip, H., Avagyan, A., Karakhanian, A.S., Ritz, J.F. & Rebai, S., 2001. Estimating slip rates and recurrence intervals for strong earthquakes along an intercontinental fault: example of the Pambak-Sevan-Sunik fault (Armenia), *Tectonophysics,* **343,** 205–232.

Quittmeyer, R.C. & Jacob, K.H., 1979. Historical and modern seismicity of Pakistan, Afghanistan, northwestern India and southeastern Iran, *Bull. seism. Soc. Am.,* **69,** 773–823.

Ravaut, P., Bayer, R., Hassani, R., Rousset, D. & Al Yahya'ey, A., 1997. Structure and evolution of the northern Oman margin: gravity and seismic constraints over the Zagros-Makran-Oman collision zone, *Tectonophysics,* **279,** 253–280.

Regard, V., 2003. Variations temporelle et spatiale de la transition subduction-collision. Tectonique de la transition Zagros-Makran (Iran) et modélisation analogique, PhD thesis, Université Aix-Marseille III, Marseille.

Ricou, L.E., Braud, J. & Brunn, J.H., 1977. Le Zagros, *Mém. h. sér. Soc. géol. Fr.,* **8,** 33–52.

Savage, J. & Burford, R., 1973. Geodetic determination of relative plate motion in Central California, *J. geophys. Res.,* **95,** 4873–4879.

Sella, G.F., Dixon, T.H. & Mao, A., 2002. REVEL: a model for recent plate velocities from space geodesy, *J. geophys. Res.,* **107**(B4), ETG 11–1, 11–32.

Sengör, A.M.C., 1990. A new model for the late Paleozoic-Mesozoic tectonic evolution of Iran and implications for Oman, in *The Geology and Tectonics of the Oman Region*, pp. 797–831, Geological Society of London Special Publication.

Shen, Z., Wang, M., Li, Y., Jackson, D.D., Yin, A., Dong, D. & Fang, P., 2001. Crustal deformation along the Altyn Tagh fault system, western China, from GPS, *J. geophys. Res.,* **106**(12), 30 607–30 621.

Stöcklin, J., 1968. Structural history and tectonics of Iran: a review, *Am. Ass. Petrol. Geol. Bull.,* **52,** 1229–1258.

Stöcklin, J., 1974. Possible ancient continental margins in Iran, in *The Geology of Continental Margins*, pp. 873–887, eds Burk, C.A. & Drake, C.L., Springer-Verlag, New York.

Talebian, M. & Jackson, J.A., 2002. Offset on the Main Recent Fault of the NW Iran and implications for the late Cenozoic tectonics of the Arabia-Eurasia collision zone, *Geophys. J. Int.,* **150,** 422–439.

Tatar, M., Hatzfeld, D., Martinod, J., Walpersdorf, A., Ghafori-Ashtiany, M. & Chéry, J., 2002. The present-day deformation of the central Zagros from GPS measurements, *Geophys. Res. Lett.,* **29**(19), 1927, doi: 10.1029/2002GL015427.

Tchalenko, J.S. & Braud, J., 1974. Seismicity and structure of the Zagros (Iran): the Main Recent Fault between 33° and 35°N, *Phil. Trans. R. Soc. Lond.,* **277**(1262), 1–25.

Tirrul, R., Bell, I.R., Griffis, R.J. & Camp, V.E., 1983. The Sistan suture zone of eastern Iran, *Geol. Soc. Am. Bull.,* **94,** 134–150.

Trifonov, V.G., 1978. Late Quaternary tectonic movements of the western and central Asia, *Geol. Soc. Am. Bull.,* **89,** 1059–1072.

Vigny, C., Socquet, A., Rangin, C., Chamot-Rooke, N., Pubellier, M., Bouin, M.-N., Bertrand, G. & Becker, M., 2003. Present-day crustal deformation around Sagaing fault, Myanmar, *J. geophys. Res.,* **108**(B11), 2533, doi:10.1029/2002JB001999.

Walker, R. & Jackson, J.A., 2002. Offset and evolution of the Gowk fault, S.E. Iran: a major intra-continental strike-slip system, *J. Struct. Geol.,* **24,** 1677–1698.

Wang, Q. *et al.*, 2001. Present-day crustal deformation in China by Global Positioning System measurements, *Science,* **294,** 574–577.

Wdowinski, S., Bock, Y., Forrai, Y., Melzer, Y. & Baer, G., 2001. The GIL network of continuous GPS monitoring in Israel for geodetic and geophysical applications, *Israel J. Earth Sci.,* **50,** 39–47.

Wells, D.L. & Coppersmith, K.J., 1994. New empirical relationships among magnitude, rupture length, rupture width, rupture area, and surface displacement, *Bull. seism. Soc. Am.,* **84**(4), 974–1002.

Wessel, P. & Smith, W.H.F., 1995. New version of the generic mapping tools released, *EOS, Trans. Am. geophys. Un.,* **76,** 329.

White, R.S., 1982. Deformation of the Makran accretionary sediment prism in the Gulf of Oman, in *Trench-Forearc Geology: Sedimentation and Tectonics on Modern and Ancient Active Plate Margins*, pp. 357–372, ed. Leggett, J.K., Geological Society of London Special Publication.

White, R.S. & Louden, K.E., 1982. The Makran continental margin: structure of a thickly sedimented convergent plate boundary, in *Studies in Continental Margin Geology*, pp. 499–518, eds Watkins, J.S. & Drake, C.L., American Association of Petroleum Geologists Memoir Tulsa, OK, USA.

Wright, T., Parsons, B. & Fielding, E., 2001. Measurement of interseismic strain accumulation across the North Anatolian Fault by satellite radar interferometry, *Geophys. Res. Lett.,* **28**(10), 2117–2120.

Zhang, J., Bock, Y., Johnson, H., Fang, P., Williams, S., Genrich, J., Wdowinsky, S. & Behr, J., 1997. Southern California Permanent GPS Geodetic Array: Error analysis of daily position estimates and site velocities, *J. geophys. Res.,* **102,** 18 035–18 055.

Zonenshain, L.P. & Le Pichon, X., 1986. Deep basins of the Black sea as remnants of Mesozoic back-arc basins, *Tectonophysics,* **123,** 181–211.